AD-A268 176

CR 93.002

NCEL

Contract Report

June 1993

An Investigation Conducted by
Adaptive Research Corporation
Huntsville, AL

STRUCTURED FINITE VOLUME MODELING
OF U.S. NAVY AIRCRAFT ENGINE TEST CELLS

TASK 1: TURBOSHAFT ENGINE -

FINAL REPORT - VOLUME 1

DTIC
ELECTE
AUG 12 1993
B

Abstract   Volume 1, Final Report, presents results of the numerical simulation of a U.S. Naval turboshaft test cell facility. The ultimate purpose of this simulation was to provide the Navy with a numerical model to be used for the evaluation of the aerothermal performance of test cells. This simulation was performed using the structured finite volume (SFV) computer code. A description of the physical model, mathematical details, boundary conditions, and results of the study are presented and covered in this report.

Volume 2, Code Documentation and Listings, provides a copy of the input files developed for the modeling of turboshaft test cells.

93-18640

METRIC CONVERSION FACTORS

Approximate Conversions to Metric Measures

Symbol	When You Know	Multiply by	To Find	Symbol
		LENGTH		
in	inches	*2.5	centimeters	cm
ft	feet	30	centimeters	cm
yd	yards	0.9	meters	m
mi	miles	1.6	kilometers	km
		AREA		
in²	square inches	6.5	square centimeters	cm²
ft²	square feet	0.09	square meters	m²
yd²	square yards	0.8	square meters	m²
mi²	square miles	2.6	square kilometers	km²
	acres	0.4	hectares	ha
		MASS (weight)		
oz	ounces	28	grams	g
lb	pounds	0.45	kilograms	kg
	short tons (2,000 lb)	0.9	tonnes	t
		VOLUME		
tsp	teaspoons	5	milliliters	ml
Tbsp	tablespoons	15	milliliters	ml
fl oz	fluid ounces	30	milliliters	ml
c	cups	0.24	liters	l
pt	pints	0.47	liters	l
qt	quarts	0.95	liters	l
gal	gallons	3.8	liters	l
ft³	cubic feet	0.03	cubic meters	m³
yd³	cubic yards	0.76	cubic meters	m³
		TEMPERATURE (exact)		
°F	Fahrenheit temperature	5/9 (after subtracting 32)	Celsius temperature	°C

*1 in = 2.54 (exactly). For other exact conversions and more detailed tables, see NBS Misc. Publ. 286, Units of Weights and Measures, Price $2.25, SD Catalog No. C13 10 286.

Approximate Conversions from Metric Measures

Symbol	When You Know	Multiply by	To Find	Symbol
		LENGTH		
mm	millimeters	0.04	inches	in
cm	centimeters	0.4	inches	in
m	meters	3.3	feet	ft
m	meters	1.1	yards	yd
km	kilometers	0.6	miles	mi
		AREA		
cm²	square centimeters	0.16	square inches	in²
m²	square meters	1.2	square yards	yd²
km²	square kilometers	0.4	square miles	mi²
ha	hectares (10,000 m²)	2.5	acres	
		MASS (weight)		
g	grams	0.035	ounces	oz
kg	kilograms	2.2	pounds	lb
t	tonnes (1,000 kg)	1.1	short tons	
		VOLUME		
ml	milliliters	0.03	fluid ounces	fl oz
l	liters	2.1	pints	pt
l	liters	1.06	quarts	qt
l	liters	0.26	gallons	gal
m³	cubic meters	35	cubic feet	ft³
m³	cubic meters	1.3	cubic yards	yd³
		TEMPERATURE (exact)		
°C	Celsius temperature	9/5 (then add 32)	Fahrenheit temperature	°F

°F   -40   0   32   40   80   98.6   120   160   200   212
°C   -40   -20   0   20   37   40   60   80   100

DISCLAIMER NOTICE

THIS DOCUMENT IS BEST QUALITY AVAILABLE. THE COPY FURNISHED TO DTIC CONTAINED A SIGNIFICANT NUMBER OF COLOR PAGES WHICH DO NOT REPRODUCE LEGIBLY ON BLACK AND WHITE MICROFICHE.

REPORT DOCUMENTATION PAGE

Public reporting burden for this collection of information is estimated to average 1 hour per response, including the time for reviewing instructions, searching existing data sources, gathering and maintaining the data needed, and completing and reviewing the collection of information. Send comments regarding this burden estimate or any other aspect of this collection information, including suggestions for reducing this burden, to Washington Headquarters Services, Directorate for Information and Reports, 1215 Jefferson Davis Highway, Suite 1204, Arlington, VA 22202-4302, and to the Office of Management and Budget, Paperwork Reduction Project (0704-0188), Washington, DC 20503.

1. AGENCY USE ONLY (Leave blank)	2. REPORT DATE	3. REPORT TYPE AND DATES COVERED
	June 1993	Final; December 1990 - September 1992

4. TITLE AND SUBTITLE STRUCTURED FINITE VOLUME MODELING OF U.S. NAVY AIRCRAFT ENGINE TEST CELLS TASK 1: TURBOSHAFT ENGINE - FINAL REPORT - VOLUME 1

5. FUNDING NUMBERS

PR - 0604215N
C - N47408-91-C-1228
DN - 661008

6. AUTHOR(S)

P. L. Daley and W. A. Mahaffey

7. PERFORMING ORGANIZATION NAME(S) AND ADDRESSE(S)

Adaptive Research Corporation
4960 Corporate Drive, Suite 100-A
Huntsville, AL 35805

8. PERFORMING ORGANIZATION REPORT NUMBER

CR 93.002

9. SPONSORING/MONITORING AGENCY NAME(S) AND ADDRESSE(S)

Commander / Naval Civil Engineering Laboratory
Naval Air Systems Command 560 Laboratory Drive
Code 09Y Facilities Systems Division/L53
Washington, DC 20362-5101 Port Hueneme, CA 93043-4328

10 SPONSORING/MONITORING AGENCY REPORT NUMBER

11. SUPPLEMENTARY NOTES

12a. DISTRIBUTION/AVAILABILITY STATEMENT

Approved for public release; distribution is unlimited.

12b. DISTRIBUTION CODE

13. ABSTRACT (Maximum 200 words)

This report presents results of the numerical simulation of a U.S. Naval turboshaft test cell facility. The ultimate purpose of this simulation was to provide the Navy with a numercial model to be used for the evaluation of the aerothermal performance of test cells. This simulation was performed using the structured finite volume (SFV) computer code. A description of the physical model, mathematical details, boundary conditions, and results of the study are presented and covered in Volume 1.

Volume 2, Code Documentation and Listings, provides a copy of the input files developed for the modeling of turboshaft test cells.

14. SUBJECT TERMS

Computational fluid dynamics, test cells, aviation test facilities

15. NUMBER OF PAGES 59

16. PRICE CODE

17. SECURITY CLASSIFICATION OF REPORT	18. SECURITY CLASSIFICATION OF THIS PAGE	19. SECURITY CLASSIFICATION OF ABSTRACT	20. LIMITATION OF ABSTRACT
Unclassified	Unclassified	Unclassified	UL

TABLE OF CONTENTS

LIST OF FIGURES

1. INTRODUCTION

1.1 Purpose of the Report

This report describes the development and applications of a computer model that simulates steady flow inside a turboshaft engine test facility. This model was developed using the Structured Finite Volume (SFV) code [1,2], a general purpose computational fluid dynamics (CFD) code. The report provides details of the mathematical model and reviews the results obtained from the computations. This work was undertaken by Adaptive Research Corporation, for the Naval Facilities Engineering Command, under Contract Number N47408–91–C–1228.

1.2 Background

U. S. Navy aircraft engines completing maintenance or repair are operated in test cells where they must meet performance specifications before reinstallation. Test cells are fully enclosed, sound absorbing hangers. The principle function of these facilities is to provide repeatable, specific test conditions. In the process, the test cells must attenuate the jet and propeller noise sufficiently for personal to carry out normal activities near the facility, cool and control the engine exhaust flow to the point that cell components are not damaged, and meet environmental standards.

The Navy has recently completed construction of the prototypes of a new generation of test cells designed for turboshaft and turboprop engines. These test cells, located at the Marine Corps Air Facility, Camp Pendleton, California, are scheduled to begin operating shortly.

1.3 Objective of the Study

The objective of this work is to provide a computational fluid dynamics model, employing the SFV code, of these prototype engine test cells for use in performance evaluation and for troubleshooting.

DTIC QUALITY INSPECTED 3

1.4 Outline of the Report

This report consists of six main sections. Following this introduction, Section 2 presents the geometric details of the turboshaft test cell along with operation conditions. Next, Section 3 contains information about the mathematical basis of the numerical model. In Section 4 the numerical details of the model such as boundary conditions are presented. The results of the present study are presented in Section 5 and the conclusions drawn are given in the final section.

2. DESCRIPTION OF THE SIMULATED PROCESS

2.1 Geometry

Details of the geometry are provided in Appendix A. The test bay is rectangular. The engine, without the rotor, is mounted on a cart and aligned with the dynamometer exhaust stack and the augmenter tube. Also on the cart is an air dynamometer which is attached by a shaft to the engine. Air for the engine and for the dynamometer enters the cell through two rows of acoustic vanes located in the front wall of the test bay. These vanes are not arranged symmetrically, and the location of the engine does not fall along the center line of the test cell. Engine exhaust, along with some cooler test bay air entrained by the jet, leaves the facility through the augmenter tube, discharging to a chimney and then to the atmosphere. The dynamometer has its own exhaust system. Both the chimney and the dynamometer exhaust stack are provided with two rows of acoustic baffles.

2.2 Operation Conditions

The engine considered in this modeling effort is the T700 turboshaft engine manufactured by General Electric. The operation conditions for the engine are listed in Table 1.

For the dynamometer, a mass flow of 14.0 lb/s (6.35 kg/s) was used. The average exit temperature used for the dynamometer was 413 F (212 C). The ambient conditions outside the cell were 29.91 mm Hg (1.013×10^5 N/m^2), 77 F (25 C), and a dry bicomponent atmosphere (76.83 wt per cent N_2).

TABLE 1. T700 Turboshaft Engine Operating Conditions

Exhaust Flow	11.2 lb/s
	5.08 kg/s
Fuel Flow	0.222 lb/s
	0.101 kg/s
Average Exit Temperature	1200 F
	650 C
Exhaust Composition (wt%)	0.7512 N_2
	0.1548 O_2
	0.0690 CO_2
	0.0250 H_2O

3. MATHEMATICAL FORMULATION

3.1   The Structured Finite Volume (SFV) Mathematical Formulation

The SFV computer code is a general–purpose CFD code in wide use throughout government, industry, and academia. It can model two– or three–dimensional, laminar or turbulent, single– or two–phase fluid flows in arbitrary geometric flow domains. SFV solves the conservation equations for mass, momentum, and energy. The details of this solution procedure follow.

3.1.1   The Governing Equations

The flow field in a given geometry can be described by the conservation equations for mass, momentum, and energy. These equations can be expressed in the following form

$$\frac{\partial}{\partial T} + \nabla \left(\rho \nabla \right) = 0 \tag{1}$$

$$\frac{\partial (\rho \nabla)}{\partial t} + \nabla \left(\rho \nabla \nabla \right) = - \nabla p + \nabla \left(\mu_{eff} \nabla \nabla \right) \tag{2}$$

$$\frac{\partial (\rho \nabla)}{\partial t} + \nabla \left(\rho \nabla h \right) = \nabla \overline{q} + \mu_{eff} \phi + \frac{\partial p}{\partial t} + \nabla \nabla P \tag{3}$$

where

∇	–	is the time–mean velocity;
ρ	–	is the gas density;
p	–	is the static pressure;
μ_{eff}	–	is the "effective" viscosity;'
h	–	is the enthalpy;
$\overline{q}$	–	is the diffusive energy flux; and
ϕ	–	is the dissipation function.

5

The effective viscosity is defined by the relation

$$\mu_{eff} = \mu + \mu_t \quad ; \quad \mu_t = C_\mu \rho \frac{k^2}{\epsilon}$$

where μ is the molecular viscosity and μ_t, the turbulent viscosity, is deduced by employing a turbulence model. SFV employs the two—equation $k-\epsilon$ turbulence model [3]. This treatment of turbulence requires the solution of two additional partial differential equations

$$\frac{\partial(\rho k)}{\partial t} + \nabla(\rho \nabla K) = \nabla\left[\frac{\mu_{eff}}{\sigma_k} \nabla k\right] + P_k - \rho\epsilon \qquad (4)$$

$$\frac{\partial(\rho\epsilon)}{\partial t} + \nabla(\rho\nabla\epsilon) = \nabla\left[\frac{\mu_{eff}}{\sigma_\epsilon} \nabla\epsilon\right] + \frac{\epsilon}{k}\left[C_1 P_k - \rho C_2\epsilon\right] \qquad (5)$$

where

k	— is the turbulence kinetic energy;
ϵ	— is the dissipation rate of turbulence kinetic energy;
$C_1, C_2, \sigma_\epsilon, \sigma_k$	— are model constants; and
P_k	— is the volumetric production rate of k, defined by

$$P_k = \mu_t\left[\frac{\partial V_i}{\partial x_j} + \frac{\partial V_j}{\partial x_i}\right]\frac{\partial V_i}{\partial x_j}.$$

When single—phase three—dimensional flow is under consideration, the dependent variables that require solution are

p	— the static pressure;
u	— the horizontal—direction velocity component;
v	— the vertical—direction velocity component;
w	— the axial—direction velocity component;
k, ϵ	— turbulence quantities (described above);
h	— the static enthalpy;

6

C1   — the mass fraction of engine gases; and

C2   — the mass fraction of dynamometer gases.

3.1.2   General Form of the Governing Equations

The governing equation for each dependent variable can be reduced to a single general form which can be succinctly represented in vector notation as

$$\frac{\partial(\rho\varphi)}{\partial t} + \nabla\left[\rho\nabla\varphi + J_\varphi\right] = S_\varphi \qquad (6)$$

The source term S_φ includes both sources and sinks of φ plus any other terms beyond those which appear on the left–hand side of the equation.

Because of the generality of the SFV code, a standard gradient–diffusion law is provided for the diffusion flux, namely

$$J_\varphi = -\Gamma_\varphi\nabla\varphi \qquad (7)$$

Where diffusion of the conserved quantities does not follow the standard form of Equation 7, compensating terms are added to the source term S_σ. In that equation, Γ_φ is the exchange coefficient for the variable φ, defined as

$$\Gamma_\varphi = \frac{\mu_{eff}}{\sigma_{\varphi,eff}} \qquad (8)$$

where $\sigma_{\varphi,eff}$ is the effective Prandtl/Schmidt number governing diffusive transport of the variable φ.

The exception to the general form given by Equation 6 is the continuity (mass conservation) equation. The pressure, p, has been classified as a dependent variable, but does not appear as the subject of a transport equation. Instead, the pressure is associated with the continuity equation which can be manipulated to derive a pressure–correction equation. SFV employs a variant of the SIMPLE pressure–correction procedure [4]. The transport coefficient Γ_φ and source term S_φ are provided for each dependent variable in Table 2.

TABLE 2. Transport Equations and Turbulence Model Constraints

	φ	Γ_φ	S_φ
Continuity Momentum:	1	0	0
x–direction	u	μ_{eff}	$-\frac{\partial p}{\partial x}$
y–direction	v	μ_{eff}	$-\frac{\partial p}{\partial y}$
z–direction	w	μ_{eff}	$-\frac{\partial p}{\partial z}$
Kinetic Energy	k	$\frac{\mu_t}{\sigma_k}$	$P_k - \rho\epsilon$
Dissipation Rate	ϵ	$\frac{\mu_t}{\sigma_\epsilon}$	$\frac{\epsilon}{k}(C_1 P_k - C_2 \rho\epsilon)$
Enthalpy	h	$(\frac{\mu}{\sigma} + \frac{\mu_t}{\sigma_t})$	0
Concentration	C	$(\frac{\mu}{\sigma} + \frac{\mu_t}{\sigma_t})$	0

$C\mu = 0.09$, $\qquad C_1 = 1.44$, $\qquad C_2 = 1.92$, $\qquad \sigma_k = 1.0$, $\qquad \sigma_\epsilon = 1.314$

3.1.3   General Form of the Finite–Domain Equations

Integration of the generalized conservation equation (6) yields a finite–difference analog for each dependent variable φ, for each control cell into which the flow geometry is divided. The integration process is carried out, and the terms in the finite–domain equations are

assembled in the manner described in many standard texts on numerical analysis [5]. For each simulation performed, the SFV program will assemble and then solve a set of simultaneous coupled equations of the general form (for point P)

$$a_P \varphi_P = a_E \varphi_E + a_W \varphi_W + a_N \varphi_N + a_S \varphi_S + a_H \varphi_H + a_L \varphi_L + S_\varphi$$

(9)

where the subscripts E, W, N, S, H, and L represent the neighbor points in space. The coefficients, a_N and others, represent the effects of convection and diffusion. S_φ is the linearized source term. The central coefficient a_P is defined as

$$a_P = a_E + a_W + a_N + a_S + a_H + a_L \tag{10}$$

The set of equations (9) are assembled and solved for each dependent variable in sequence. The solution of the flow field then proceeds iteratively to steady–state.

3.1.4   Auxiliary Relations

To complete the mathematical formulation of a problem the specification of additional information is required: namely, fluid properties and boundary conditions.

SFV allows the arbitrary specification of fluid properties. The models resulting from this study will employ fluid properties typical of the conditions present in the Camp Pendleton test cells. SFV also allows several different types of flow and thermal boundary conditions. These will be appropriately chosen so as not to sacrifice the fidelity of the models and also to allow for easy modification in the course of the parametric studies.

4. NUMERICAL DETAILS AND PHYSICAL MODELS

4.1 Introduction

This section of the report describes the various aspects of the modeling method necessary to simulate the flow and heat transfer inside the test facility. First, the computational grid employed in this simulation is described. Next, the physical properties are defined. This is followed by a discussion of the boundary conditions used in the computational model.

4.2 Grid Description

The first step in setting up a numerical model is the specification of the computational grid. For this study a three dimensional Body—Fitted Coordinate (BFC) grid was employed. The grid for this modeling effort is quite complex. In order to simplify the grid generation, a procedure has been developed to allow for relatively easy modifications of the test cell configuration.

In this method the user specifies various geometric quantities. The standard input files then create a set of data files for the EasyMesh [6] program which is a two dimensional BFC package. The user must then run this grid generation package to create a set of two dimensional grids. The standard input files are then re—executed to produce the final grid by stacking, blending, and rotation of the two dimensional grid planes.

The final computational grid for this study is shown in Figure 1. This grid has 40 cells across the test bay, 35 cells in the vertical direction, and 77 computational cells in the axial direction. The grid is clustered in areas of geometric changes, areas of expected high shearing action, and areas of heat transfer. In Figures 2 through 4 outlines of the internal components are presented.

4.3 Properties of the Fluid

The properties of the gases mixture inside the test cell were calculated based on the local conditions. The local heat capacity was computed using the gas mass fraction and the cell

temperature using JANNAF [7] polynomial expressions. The gas density was calculated using the ideal gas law (requiring local pressure, molecular weight, and temperature). The laminar kinematic viscosity was assumed to have a constant value of 1.08×10^{-4} ft^2/s (1.0×10^{-5} m^2/s). The turbulent viscosity, which tends to dominate, was calculated from the local turbulence quantities.

Heat transfer through the augmenter tube wall required the specification of the material thermal conductivity. Inside the room the thermal conductivity of mineral fiber with a value of 0.22 Btu/ft–s–R (0.38 W/m–K), was used. In the chimney the conductivity of steel was used. The value of steel was taken to be 26 Btu/ft–s–R (45 W/m–K).

4.4 Boundary Conditions

For this model, the boundary conditions requiring specifications were

- the engine,
- the dynamometer,
- inlet into test cell,
- outlet of dynamometer stack and chimney,
- wall boundaries, and
- heat transfer through the augmenter wall.

These boundary conditions and sources are discussed in the following sections.

4.4.1 Engine

The engine is modeled as a hollow cylindrical shape with a variable cross sectional area. Inside this region a plate of computational faces were blocked. On the intake side a mass sink is applied which corresponded to the exit mass flow minus the fuel intake.

On the exhaust side a mass source was applied to account for the engine mass flow. Other boundary conditions applied the appropriate sources for the momentum, enthalpy, turbulence, and concentrations. The exit turbulence quantities were calculated assuming a

15 per cent turbulence intensity from the following equation:

$$k = 1/2\ (vI_t)$$

$$\epsilon = 0.1643\ k^{1.5}/l_m$$

where

I_t — is the turbulence intensity and

l_m — is the mixing length (based on a gap distance or inlet radius)

4.4.2   Dynamometer

Similarly for the dynamometer, a plate inside the dynamometer was blocked. On the inside face a mass sink was applied. A mass source was applied to the top face along with sources for the momentum, enthalpy, turbulence and concentrations. A turbulence intensity of 10 per cent was assumed.

4.4.3   Inlet

At the inlet a fixed pressure was applied which corresponded to the ambient pressure. From this and the other boundary conditions the mass flow was computed. Since this mass flow varies during the solution process, the momentum source was calculated from the adjusting inflow. The enthalpy and concentrations were considered to be ambient. A turbulence intensity of 2 per cent was used to calculated the incoming turbulence values. A constant velocity of 3.3 ft/s (1.0 m/s) was used in the turbulence calculations.

The baffles located at the inlet, dynameter exhaust, and chimney were not directly modeled. These effects were modeled by calculating the momentum loss through the baffles from

$$\Delta p = 0.5\ K\rho v^2$$

where

K is a loss coefficient.

12

Supplied with pressure drop across the baffles along with gas density and velocity an accurate determination of K is possible. Pressure data only existed for the baffles of the exhaust stack. However, this value was for a location inside the baffles. It was assumed that the pressure drop across the baffles was double this value. Using estimates for density and velocity a K—loss factor of 0.2 was calculated. This was lowered to 0.1 for all baffles in an effect to better predict temperature data (Section 5.4).

4.4.4 Outlet

At the two 'outlets' a fixed pressure was used. If no recirculation occurs this is all that is required as in the case of the dynamometer stack. However, in the chimney, the possibility of recirculation at the exit was extremely great. Momentum and energy sources were supplied if and when recirculation at the exit plane was calculated. The momentum source was based on the amount of mass being brought into the domain and the energy source was based on ambient gas conditions.

4.4.5 Wall Boundaries

At the wall boundaries the wall function approach [3] was used to account for momentum losses. This condition is not applied directly to the wall but rather at a point outside the viscous sublayer, where the logarithmic law of wall prevails. This is where turbulence is assumed to be in local equilibrium (i.e., the generation and dissipation of turbulence energy are equal). Heat transfer was not considered except through the augmenter tube wall.

4.4.6 Heat Transfer through Augmenter Tube

To compute the heat transfer through the augmenter tube, a composite heat transfer treatment was used. Surface heat transfer coefficients on both surfaces (inside and outside) were calculated using the standard SFV wall friction treatment. The overall heat transfer conductance between the fluid cell adjacent to the inner wall and the one adjacent to the outer wall was evaluated using these two surface coefficients (in the form of a heat transfer resistance) and the assumed thermal resistance through the tube wall. This last resistance was evaluated using a conductivity of insulation and thickness of insulation provided by the Navy. In the chimney, where there was no insulation, the conductivity and thickness of the augmenter tube wall was used for the solid contribution to the overall heat transfer conductions.

5.   DISCUSSION OF RESULTS

This report deals mainly with results from one computational run. Differences in the temperatures predicted and measured values gave rise to the investigation of various items in regard to their effect on temperature. These items will also be discussed in the following sections.

5.1   Velocity

The velocity vectors are presented in Figures 5 through 10. A cross sectional view of the vectors are show in Figure 5. This plot provides a good overall display of the major flow patterns within the calculation domain. Two plots of velocity around the dynamometer are shown in Figures 6 and 7. The first one again shows a side view. In this plot the major features of the dynamometer and engine inlet are clearly visible. This plot shows the air movement into the two 10" diameter (0.254 m) openings of the dynamometer and also the 14" diameter (0.366 m) engine inlet. This plot shows the alignment of the dynamometer with the dynamometer exhaust. In this case the dynameter is shifted 1" (0.0254 m) forward. With this alignment part of the flowing exiting the dynamometer actually enters into the dynamometer exhaust sleeve. In Figure 7 another section (X–Y) across the dynamometer is presented. In this plot note the line above the circular inlet. This is the location of the boundary conditions to account for the increase in temperature in the dynamometer. Because of the swirl in the dynamometer, the exit velocity components were supplied at a 45 degree angle. The velocity for the X and Y–direction was 59.1 ft/s (18.0 m/s).

Figure 8 shows the velocity vectors around the gap between the engine and augmenter tube. The entrainment of the surrounding gases into the tube is clearly shown. The maximum velocity of the engine is 438 ft/s (133 m/s). The velocity in the chimney section is shown in Figure 9. In the wall region the ducting changes from a circular duct into a square duct. The axial momentum propels the gases inside the augmenter tube to the aft side of the bend section. The gases do not have enough time to spread to the entire cross section of the chimney, thus causing a recirculation zone at the exit of the calculation.

The final vector plot (Figure 10) shows a top side view of the velocity vectors entering into the test cell. The entrance velocity is approximately 5 ft/s (1.5 m/s). The spreading of the incoming air and the recirculation zone beside the inlet baffles can be seen.

14

5.2   Temperature

Temperature plots are provided in Figure 11 through 19. The overall temperature field is shown in the Figure 11. The location and effect of the two heat sources can be observed. Details of the temperature field around the dynamometer are displayed in Figures 12 and 13. The exit temperature of the dynamometer used in this study was 413 F (212 C). In Figure 12 the effect of the misalignment between the dynamometer and the dynamometer sleeve can be noted. If not for the skirt, the gases would enter into the test cell with a velocity approximately the same magnitude as leaving the dynamometer. Originally no swirl was used as a boundary condition. Using this boundary condition no temperature gradient was predicted at the exit (i.e., uniform 413 F exit temperature). During additional studies described in Section 5.4, a decision was made to implement a swirling component of velocity.

The skirt channels the flow downward back into the suction of the dynamometer. The effect of the swirl at the dynamometer boundary condition can be seen in Figure 13. With this boundary condition flow is entrained on the right side (looking fore to aft) and expelled on the left side. The effect of the entrainment can be seen in the temperature plot (Figure 14) at the exit of the chimney exhaust section. This temperature range at the exit varies from 386 F to 413 F (196 C to 212 C).

The temperature around the exit of the engine is shown in Figure 15. The exit temperature of the engine was 1200 F (650 C). This temperature is then reduced as the engine gases are mixed with the entrained air in the augmenter tube as shown in Figure 16. The plot of temperature at the exit of the augmenter tube is given in Figure 17. At this point the temperatures range from 681 F to 802 F (361 C to 428 C). The average temperature is approximately 763 F (406 C). In Figure 18 the temperatures at the exit of the chimney section are plotted. The zone of recirculation is clearly noted by a region where the temperature is 77F (25 C), which corresponds to ambient conditions. An axial temperature profile plot is provided in Figure 19. In this plot the temperature at three locations falling inside the augmenter tube is shown. The near wall temperatures are shown by lines (Y—cell index) labeled 12 and 24 while the core flow of the tube is represented by line 19.

5.3 Other Quantities

In Figure 20 the pressure field located approximately 2 ft (0.6 m) from the right side is displayed. There is a cell depression through out this entire computational plane, however in terms of inches of water the values are quite small. Figure 21 shows the turbulence kinetic energy (TKE) in the gap region of the engine. Using a turbulence intensity value of 15 per cent an inlet value for TKE of 202 m^2/s^2 was obtained.

Two global numbers for the calculation were calculated. These were the pumping ratios for the dynamometer and the engine. The values calculated for this computational run were −0.067 and 0.755, respectively. The negative value for the dynamometer pumping ratio indicates that more leakage than entrainment occurred.

Heat transfer through the augmenter tube was at the rate of 1.2 BTU/s (1270 J/s). Approximately 90 per cent of this occurred in the uninsulated section in the chimney.

5.4 Comparison With Data

During October of 1991 experimental data was taken for the test case that was simulated. The results are listed in Table 3. Included in the table are the values obtained from the computation run.

TABLE 3. Summary of Experimental Results

	EXP	CFD
Pumping ratio engine	0.68	0.76
Pumping ration dynamometer	0.74	−0.07
Cell depression (in H2O)	0.15	<0.01
Engine augmenter exit average temperature (F)	618	763
Engine augmenter exit maximum temperature (F)	628	802
Engine exhaust stack average temperature (F)	555	nc*
Engine exhaust stack maximum temperature (F)	596	744
Dynamometer exhaust duct average temperature (F)	348	<400
Dynamometer exhaust duct maximum temperature (F)	362	413
Dynamometer exhaust exit maximum temperature (F)	413	413**

*Not calculated

** Boundary condition

A greater degree of confidence was given by NCEL to the actual temperature measurements than other quantities (i.e., pumping ratios, velocity measurements). The model seemed to overpredict the values of the temperatures for both the dynamometer and augmenter exists. Because of this several weeks were spent investigating the differences.

The dynamometer was the first area to be studied. Given the geometry with a gap width of only 1.25" (0.0318 m) and the misalignment of the exhaust and the stack, it was difficult to explain this amount of entrainment indicated by the data. In order to study this region a smaller 3–dimensional model was extracted from the larger model. During this study eleven computational tests were conducted to study the effect of the turbulence intensity, K–loss factor, exit velocity direction, and gap space.

Initially, no swirl was assumed as a boundary condition for the dynamometer. With this condition, no entrainment was observed (only a leakage into the test cell). Variations of the turbulence intensity and the K–loss factor produced the similar results (i.e.,, no temperature gradient at the exit). The value for the K–loss factor had a large effect on the amount of leakage between the gap. The larger the K–loss factor the greater the leakage. It was only when swirl was added to the dynamometer boundary condition that entrainment was observed. However, in all cases studied there was a negative pumping ratio, indicating more leakage than entrainment. The gap between the dynamometer exist and the exhaust was increased over several cases until it fell 0.5" (0.0127 m) below the skirt. The major result was that as the gap increase so did the amount of leakage into the test cell.

Under no condition studied did the model match the data. The average exit temperature was always higher. These findings point to explanations or combinations as to the difference. The first is, that actual geometry may not have been simulated (i.e.,, the gap was larger or a different misalignment). The second is the boundary condition used in the dynamometer. In order to rigorously model the dynamometer, momentum sources would have been supplied. With the proper sources the model would have accurately predicted the mass flow through the dynamometer. However, this would have been less stable and difficult to match the known mass flow through the dynamometer. Due to these reasons a plate location was assumed inside the dynamometer (described in Section 4.4.2). On one side of the plate a mass sink was applied, while on the top side a mass source was applied which took into account the temperature rise inside the dynamometer If this boundary

17

condition greatly overpredicts the pressure in the gap region, an under prediction of the entrained mass will occur. This can be further investigated with a small 3-dimensional model.

The exit temperatures of the augmenter tube were then studied in detail. During these studies the following four parameters were examined; engine turbulence intensity, grid resolution, K-loss of inlet and chimney, and engine temperature. The preliminary results indicated a need for a higher engine pumping ration to account for an over prediction in temperatures. The first test involved lowering of the engine turbulence intensity. The result to the pumping ration was minimal.

Grid resolution was the next item investigated. A smaller 3-dimensional area around the augmenter tube was assembled from the larger model. Two cases were conducted. The first used the same grid spacing while the second increased the number of cells in the gap region in all three directions. Preliminary results showed little difference between the pumping ratios, indicating a satisfactory level of grid refinement.

At this point, the full model was restarted with modifications to the boundary conditions namely; swirl at the dynamometer, turbulence intensity of engine increased from 8 to 15 per cent, and a lower K-loss factor for the inlet and chimney (note these are the results presented in this report). It was reasoned that by lowering the K-loss factor, more entrainment would occur as in the case of the dynamometer. However, it was found that the model is fairly insensitive to the K-loss factors used for the inlet and the chimney (i.e.. very little difference in the pumping ratio). Reducing the K-loss factor from earlier estimates to a value of 0.1 resulted in the reduction of the cell depression from 0.008 inches of H_2O to 0.004 inches of H_2O.

It was originally thought that the value of the engine turbulence intensity had little effect on the results, as indicated by the first test. A 2-dimensional model was developed by NCEL in order to investigate the temperatures within the augmenter tubes. This model showed that the mixing inside the augmenter tube was greatly affected by engine turbulence intensity, as shown in Figures 22 through 24. In these cases the inlet value of turbulence kinetic energy was increased from 65 to 520 to 977 m^2/s^2. The results show that as the intensity is increased the overall mixing inside the augmenter tube is enhanced. However, the pumping ratios only varied between 0.428 and 0.463 for the three cases. A

closer look at the data from the first test confirmed the effect of turbulence intensity on temperature gradient.

The only parameter left to explain the differences in temperatures was the value used for the engine exhaust temperature. A valve of 1200 F (650 C) had been used. This value was obtained from engine specifications and was not a measured quantity. At this time a 1–dimensional calculation was performed. In this study two streams were "mixed" simulating the mixing of engines gases and ambient air with a pumping ratio of 0.760. In order to obtain a mixture with a average temperature of 620 F (327 C), as indicated by the data, the exit engine temperature had to be 970 F (521 C) or the pumping ratio had to be increased to 1.28 (at 1200 F). The large model was repeated with the engine temperature lowered to 1030 F (554 C). Figure 25 shows the plot of temperature at the exit of the augmenter tube.

With these studies of the augmenter tube, there is no parameter that can be adjusted to increase the pumping ratio from 0.760 to 1.28. The best possible explanation for the difference in temperature is that the exit engine temperature is actually lower than the value used. If the profile is not matched, these tests indicate that the value of the turbulence intensity can be modified to increase or decrease the gradient across the exit of the augmenter tube. If the locations of the temperature probes were to be laid out over the predicted values from the model (Figure 17), it can be noted that they would generally fall in an area of average temperature of the plane. The probes are not placed in a location that will pick up the full gradient of the exit plane.

The measured and predicted results are also different in one other location. Measured velocities show that in the chimney section the flow exits the fore side. The computational model predicts that the flow exits the aft side with recirculation occurring on the fore side. Previous turn around duct studies [8] predict (and match data) the transfer of momentum to the aft side. There is no explanation for the difference in results.

6. CONCLUSION

A 3—dimensional model of a Naval test cell facility has been developed. This model allows the user to investigate various parameters of interest including variations in geometry, ambient conditions, and boundary conditions. The results of this study show

- an engine pumping ratio of 0.755;
- an dynamometer pumping ratio of −0.067;
- cell depression of less than 0.01" of water;
- an augmenter tube average temperature of 763 F; and
- an exhaust stack temperature near the value of the dynamometer exit.

Although the predicted temperatures were higher than measured values possible explanations to the differences include

- difference in modeled and actual geometries and
- types and values of boundary conditions including an unmeasured engine exit temperature.

Results of this model were sensitive to

- K—loss value for the dynamometer exhaust,
- Swirl at augmenter exit,
- Engine turbulence intensity, and
- Engine exit temperature.

Results of the model were not (or least) sensitive to

- K—loss for inlet and chimney,
- Grid refinement, and
- Heat loss through the augmenter tube.

7. REFERENCES

1. "The SFV Beginner's Guide, "Adaptive Report 100, 1992.

2. "The SFV Reference Manual", Adaptive Report 200, 1992.

3. Launder, B. E. and Spalding, D. B., _Mathematical Models of Turbulence_, Academic Press, 1972.

4. Patankar, S. V. and Spalding, D. B, "A Calculation Procedure for Heat, Mass and Momentum Transfer in Three—Dimensional Parbolic Flows," Int. Journal of Heat and Mass and Momentum Transfer in Three—Dimensional Parabolic Flows," Int. Journal of Heat and Mass Transfer, pp. 1787–1806, 1972.

5. Patankar, S. V., _Numerical Flow and Heat Transfer,_ Hemisphere, New York, 1980.

6. Daley, P. L. and Owens, S. F., "User Manual for Grid Generation Program", CHAM Report 2008/2, November 1988.

7. Gordon, S. and McBride, B., "Computer Program for Calculation of Complex Chemical Equilibrium Compositions", NASA SP–273, 1971.

8. Mahaffey, W. A. & Mukerjee, T., "PHOENICS Verification Exercise: Simulation of Cold Flow Test in Rockwell Axisymmetric Turn Around Duct", July 1989.

TURBOSHAFT TEST CELL
OUTLINE OF FEATURES
WITH DISPLAY OF GRID

PHOENICS

NCEL: TEST CELL TURBOSHAFT ENGINE
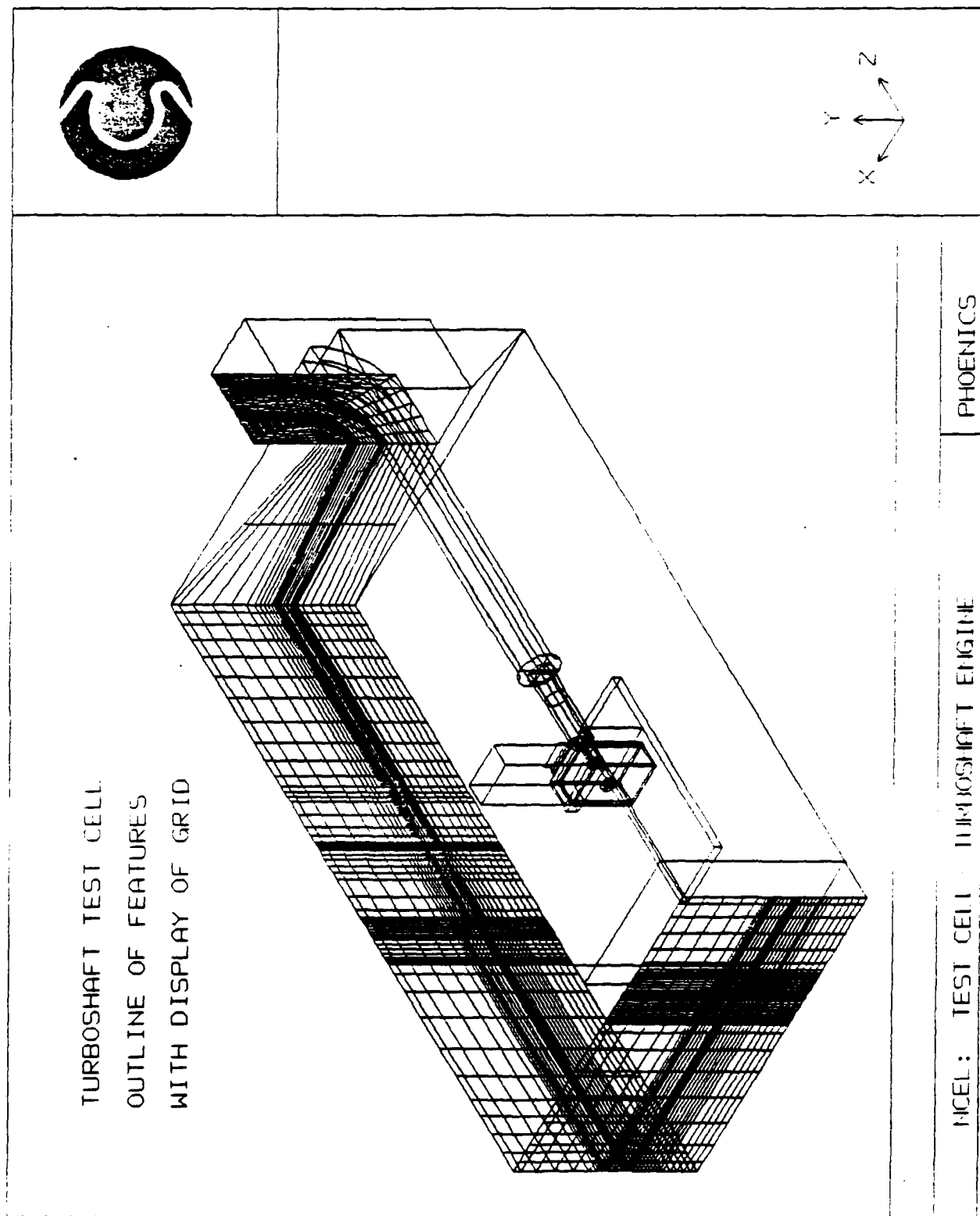
Figure 1. Computational Grid

22

TURBOSHAFT TEST CELL
OUTLINE OF FEATURES

PHOENICS

NCEL: TEST CELL - TURBOSHAFT ENGINE
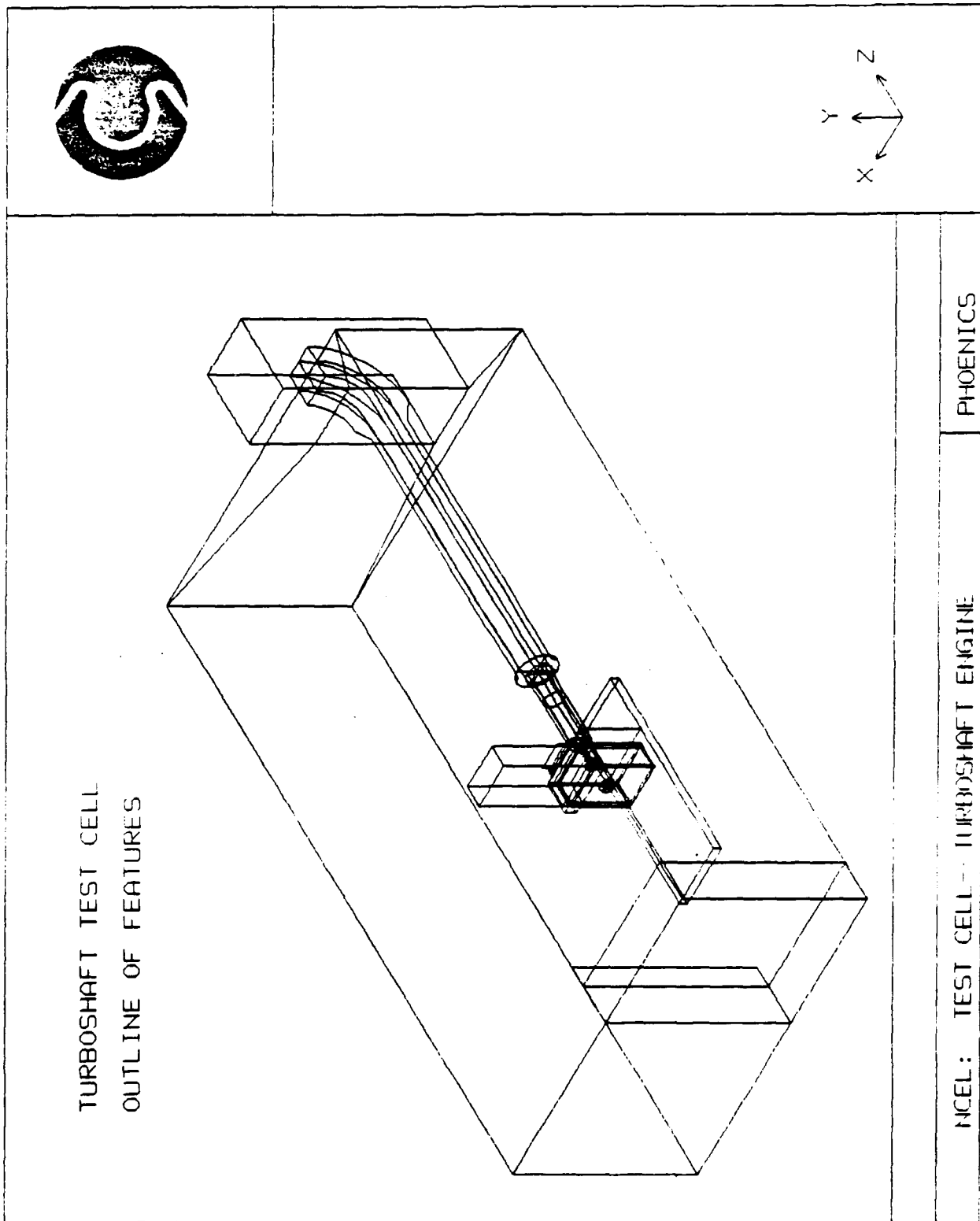
Figure 2. Outline of Features (ISO View)

23

Figure 3. Outline of Features (Side View)

TURBOSHAFT TEST CELL

OUTLINE OF FEATURES

TOP VIEW

X ← Z

PHOENICS

ICEL: TEST CELL TURBOSHAFT ENGINE
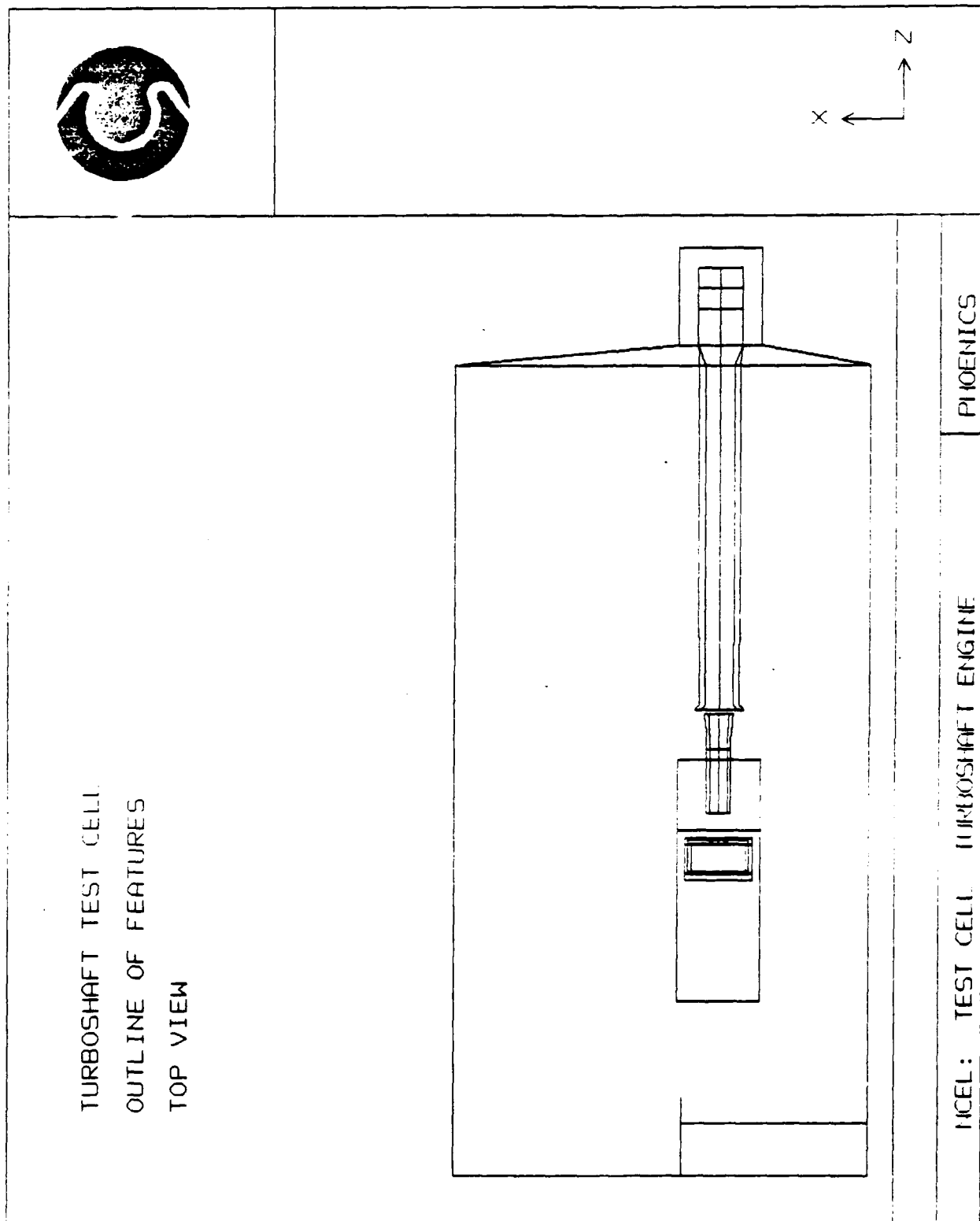
Figure 4. Outline of Features (Top View)

VELOCITY VECTORS

IX = 18

→ : 547 ft/s   Min : 0.0000E+00   Max : 4.3853E+02   PHOENICS

NCEL: TEST CELL--TURBOSHAFT ENGINE
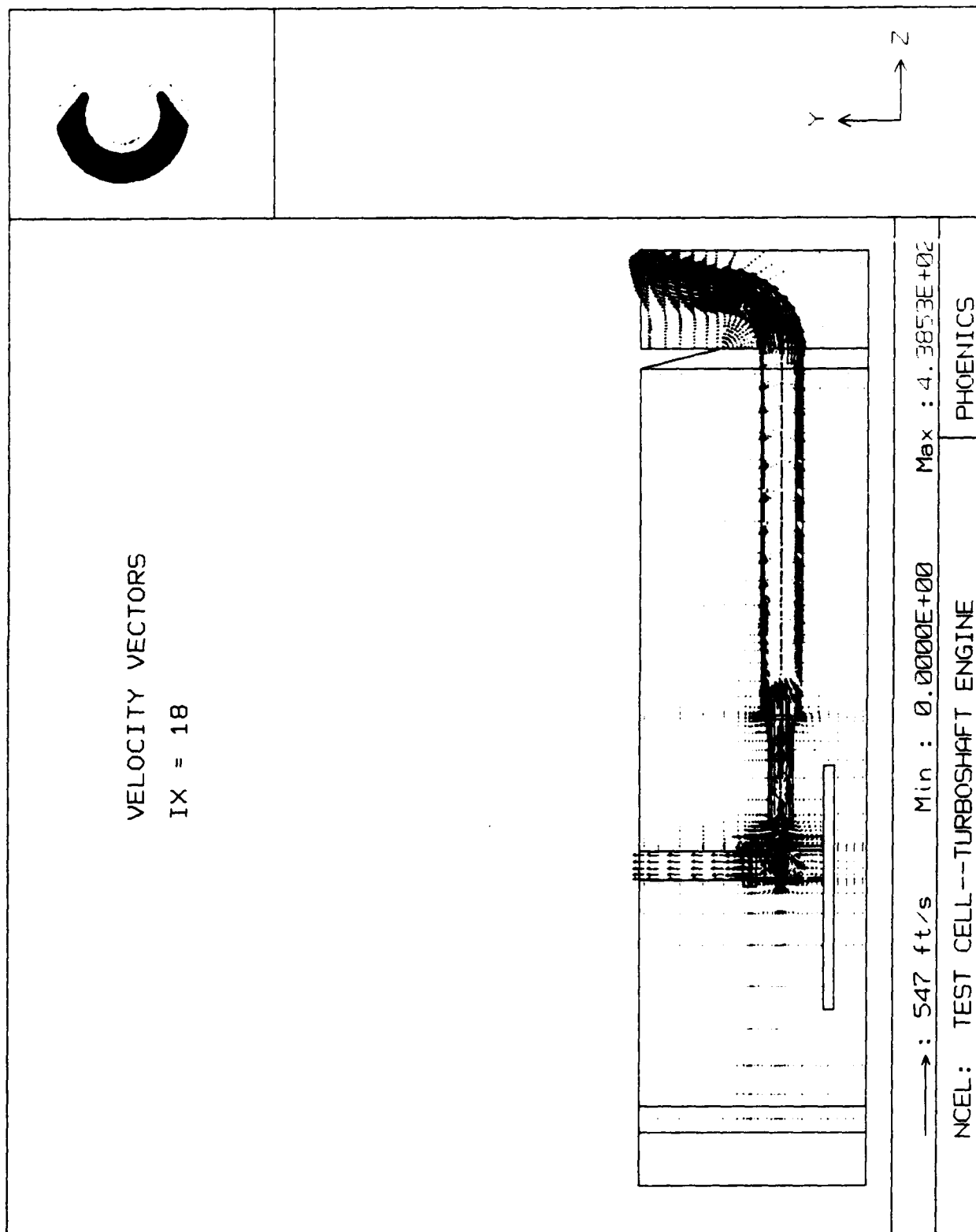
Figure 5. Velocity Vectors

26
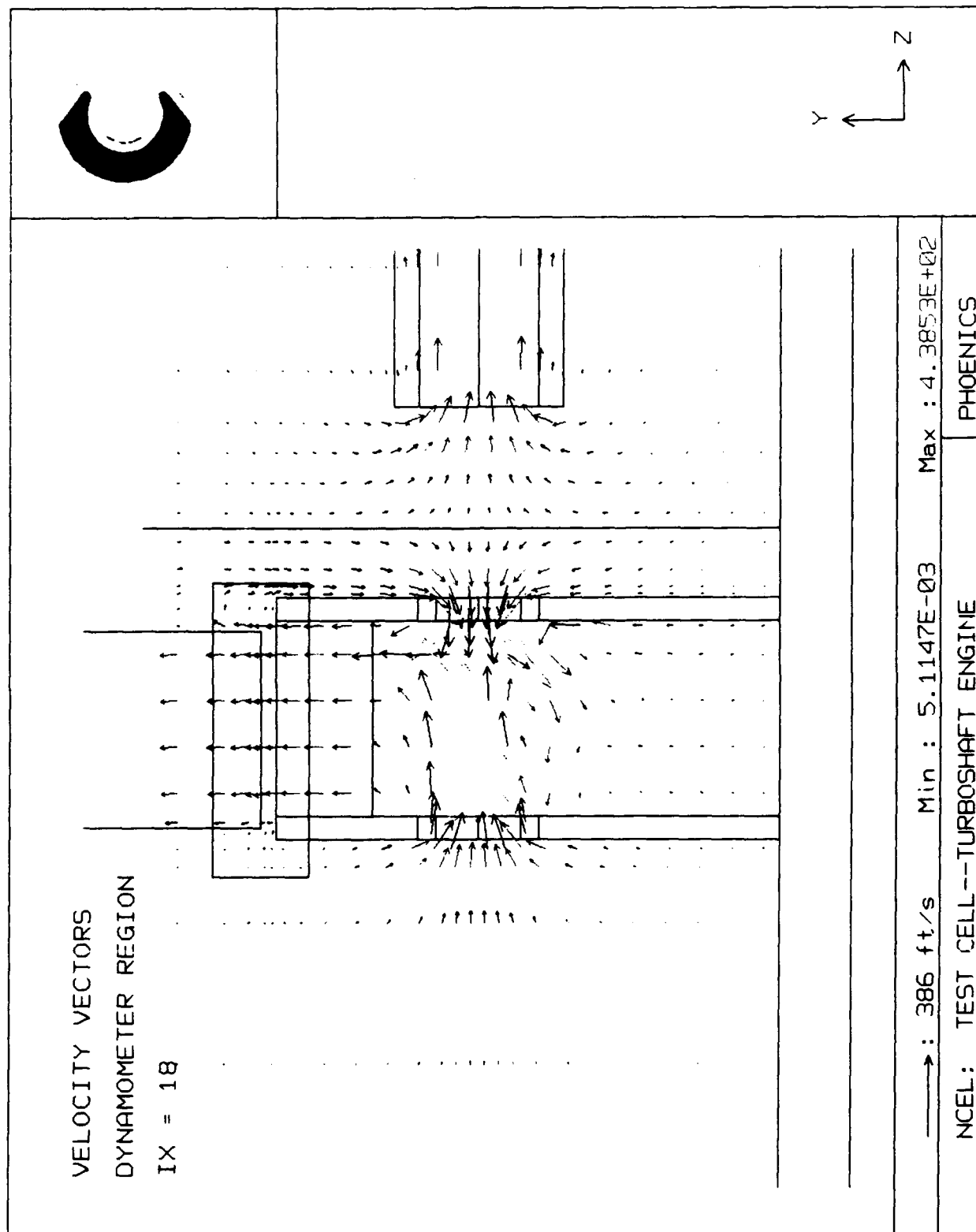
Figure 6. Velocity Vectors Dynamometer (Y-Z)
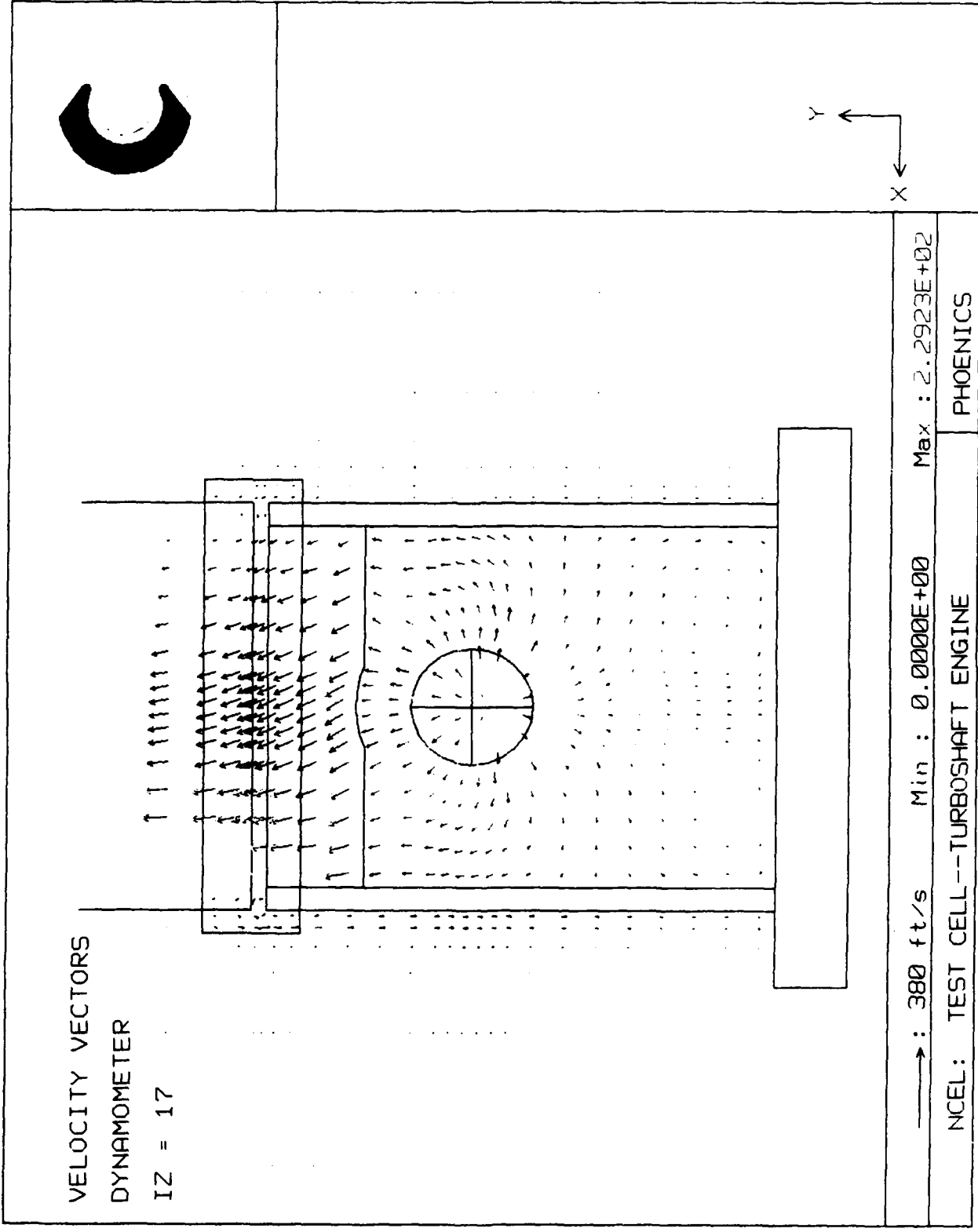
Figure 7. Velocity Vectors Dynamometer (X-Y)
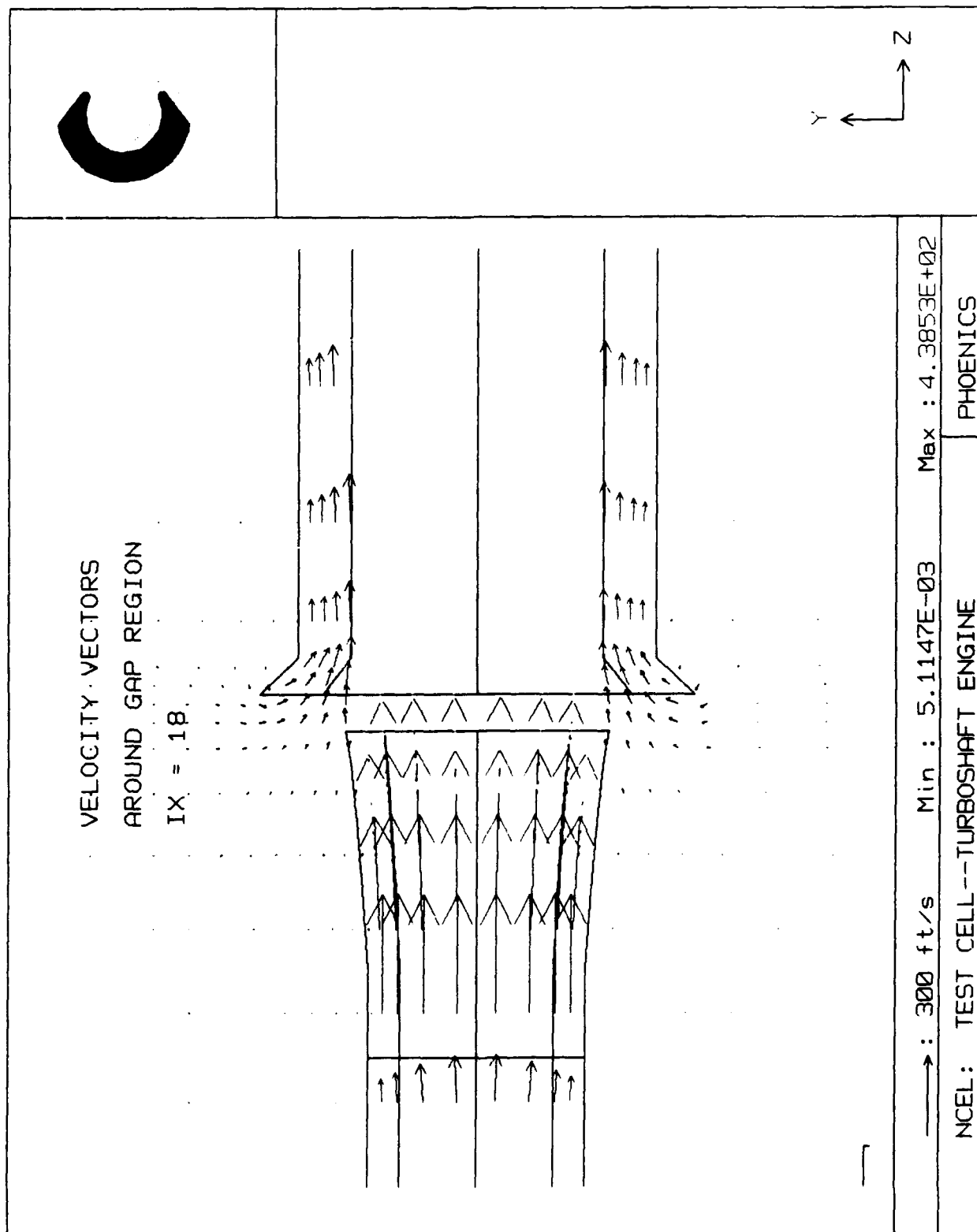
Figure 8.   Velocity Vectors Around Gap Region

29
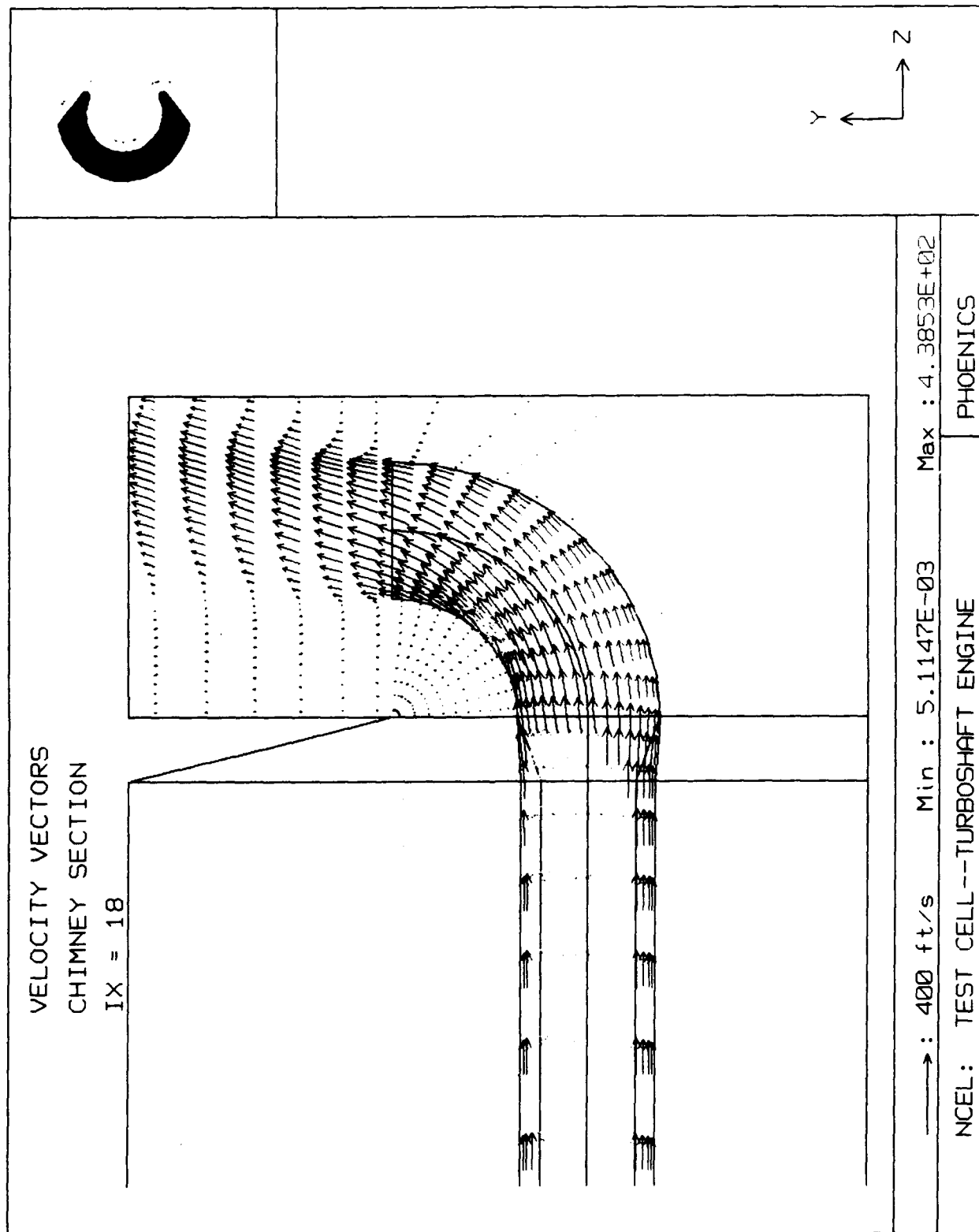
Figure 9. Velocity Vectors Chimney Section

Figure 10.   Velocity Vectors Inlet Section

TEMPERATURE

IX = 18

F
77
157
238
318
398
478
558
639
719
799
879
959
1040
1120
1200

Z

NCEL: TEST CELL—TURBOSHAFT ENGINE   PHOENICS
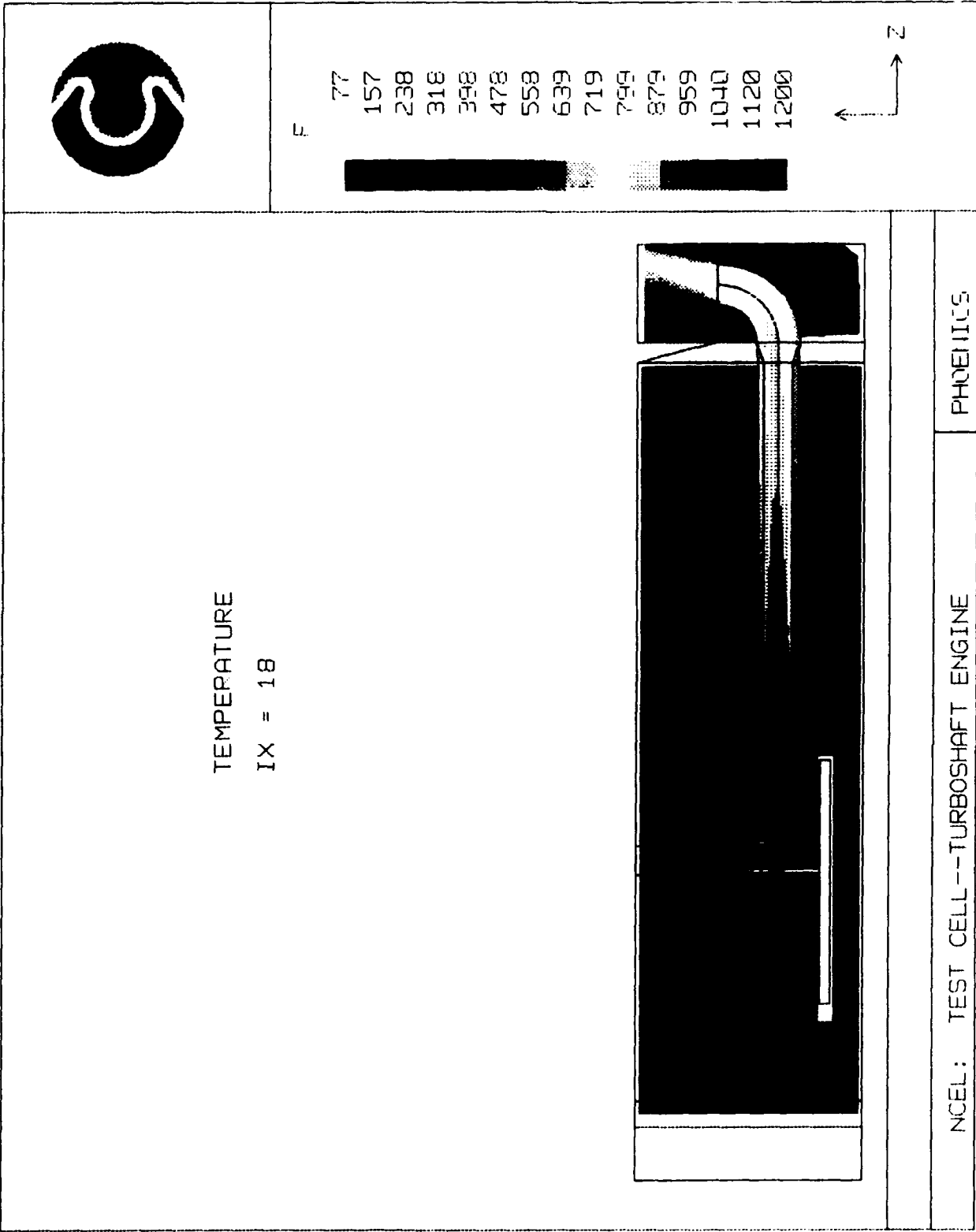
Figure 11.   Temperature
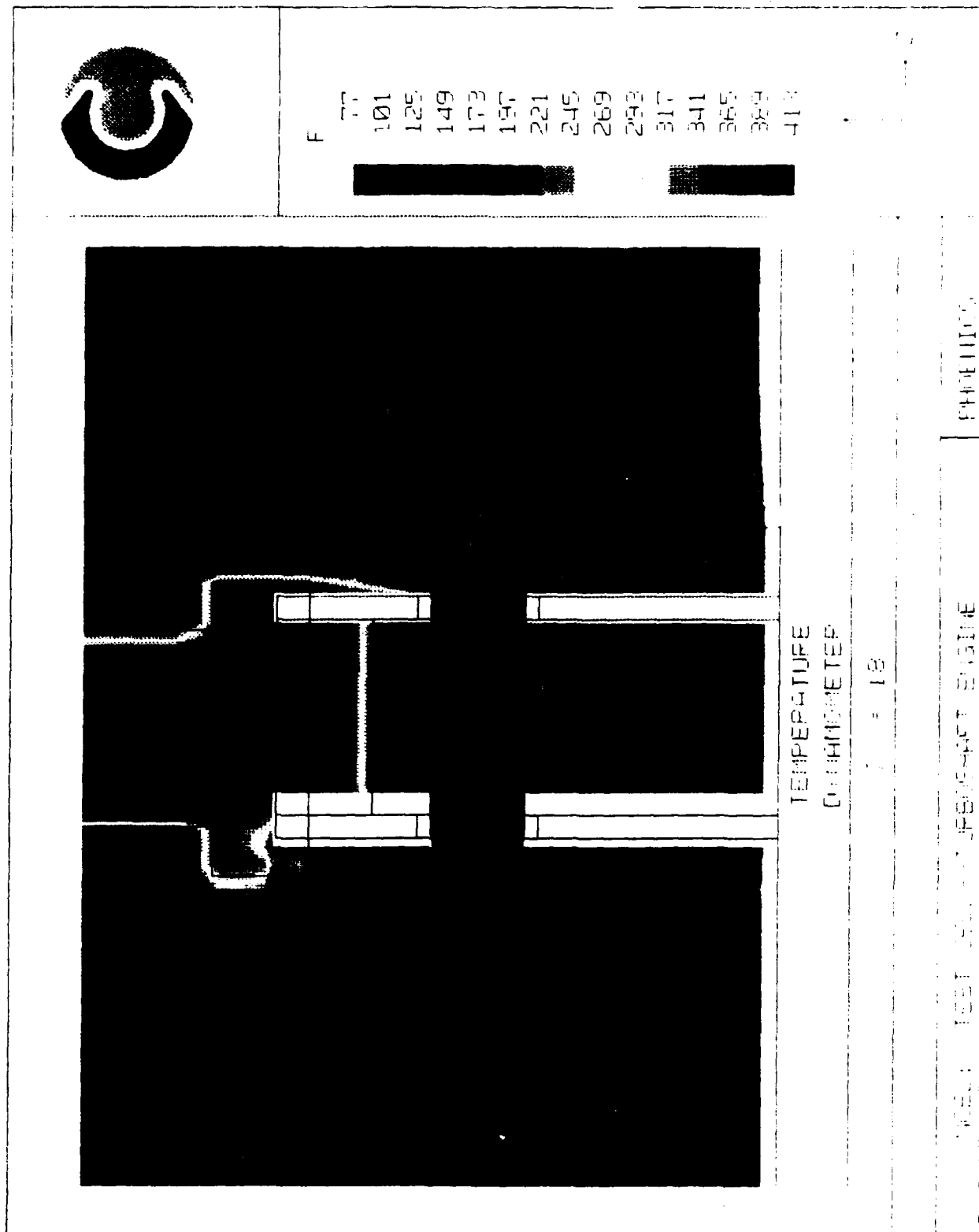
Figure 12. Temperature Dynamometer (Y-Z)
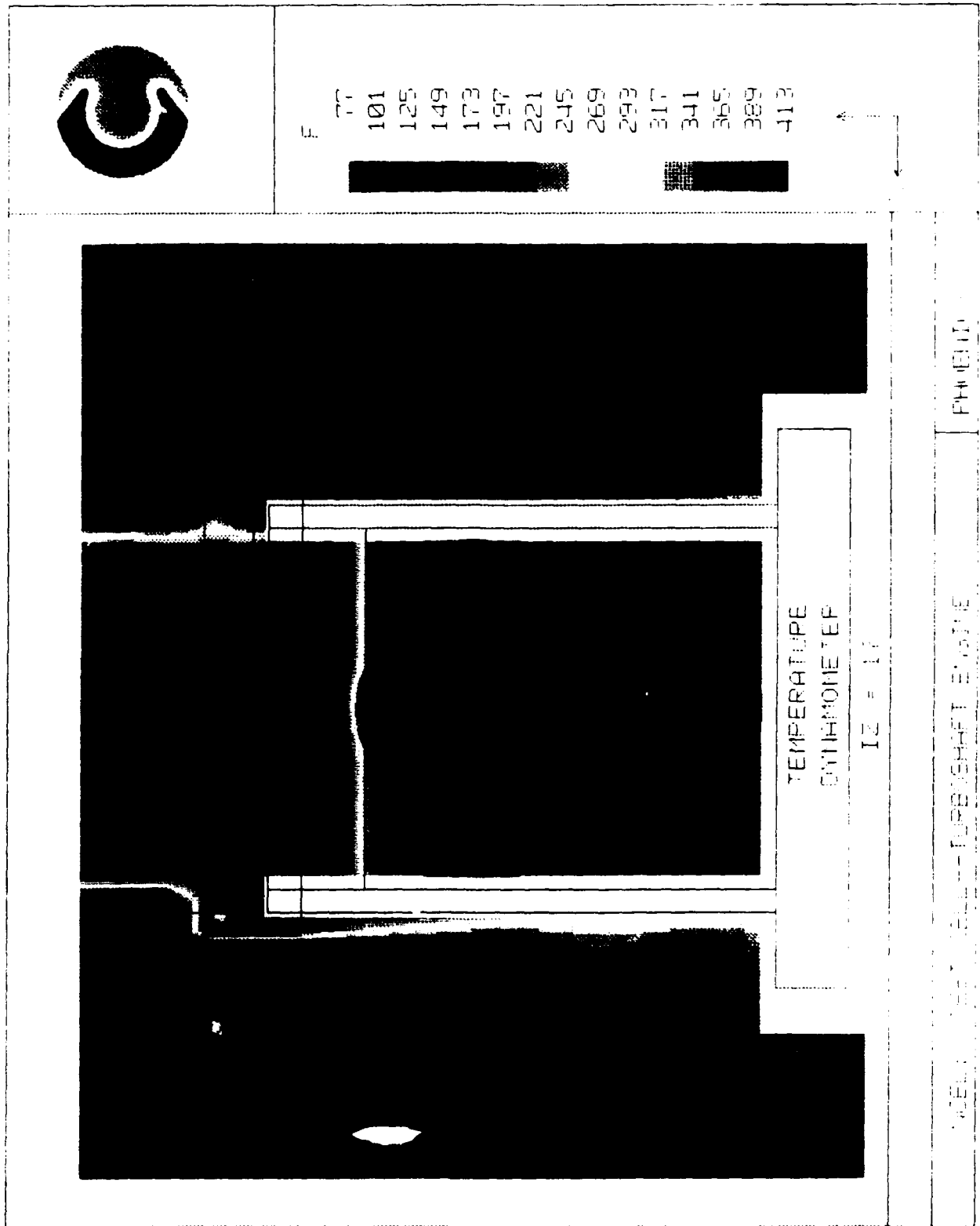
Figure 13. Temperature Dynamometer (X-Y)

34

TEMPERATURE
EXIT OF DYNAMOMETER SECTION

NY = 35

F
386
388
390
392
394
396
398
400
402
403
405
407
409
411
413

PHOENICS

NCEL: TEST CELL--TURBOSHAFT ENGINE
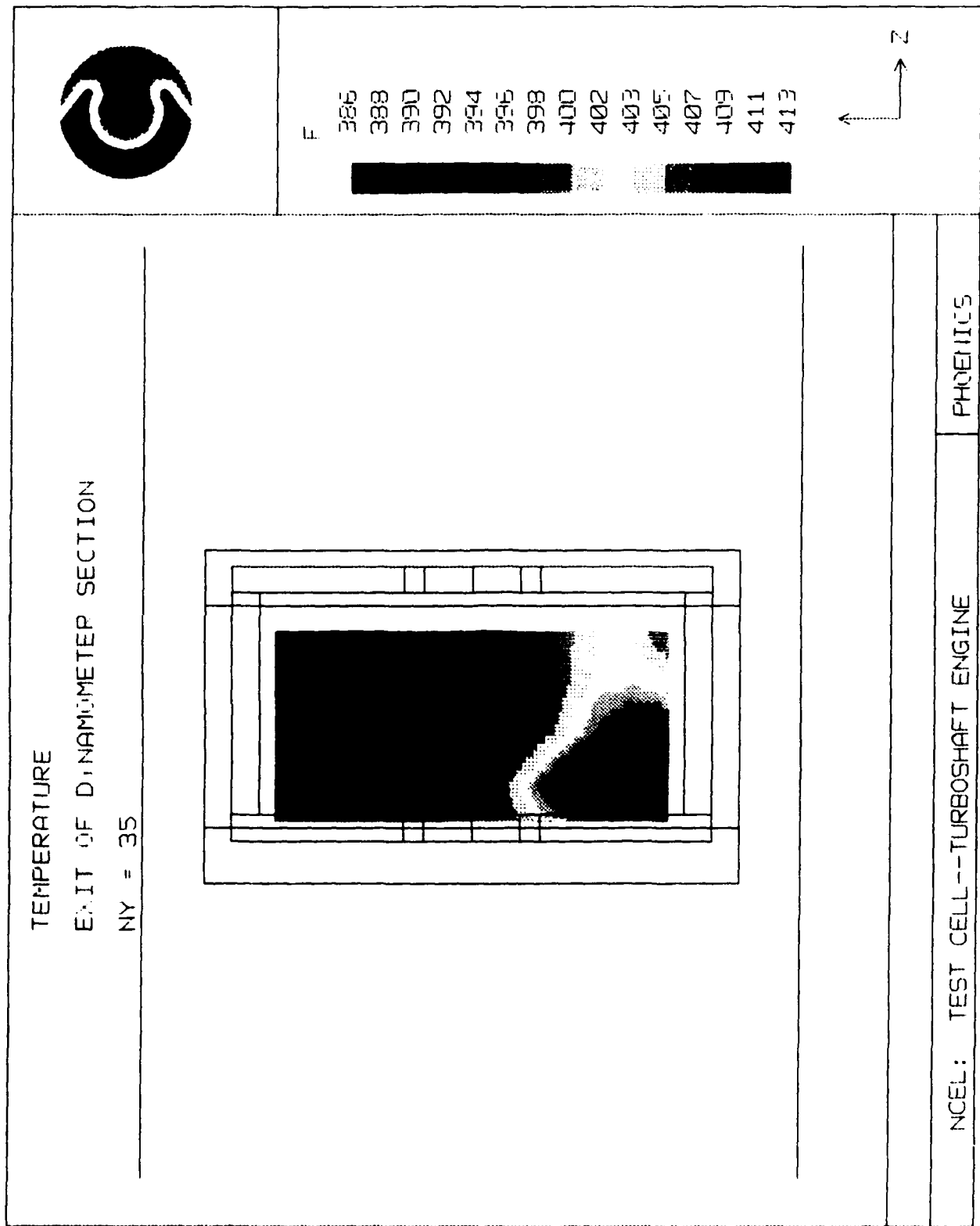
Figure 14. Temperature Exit of Dynamometer Section

35
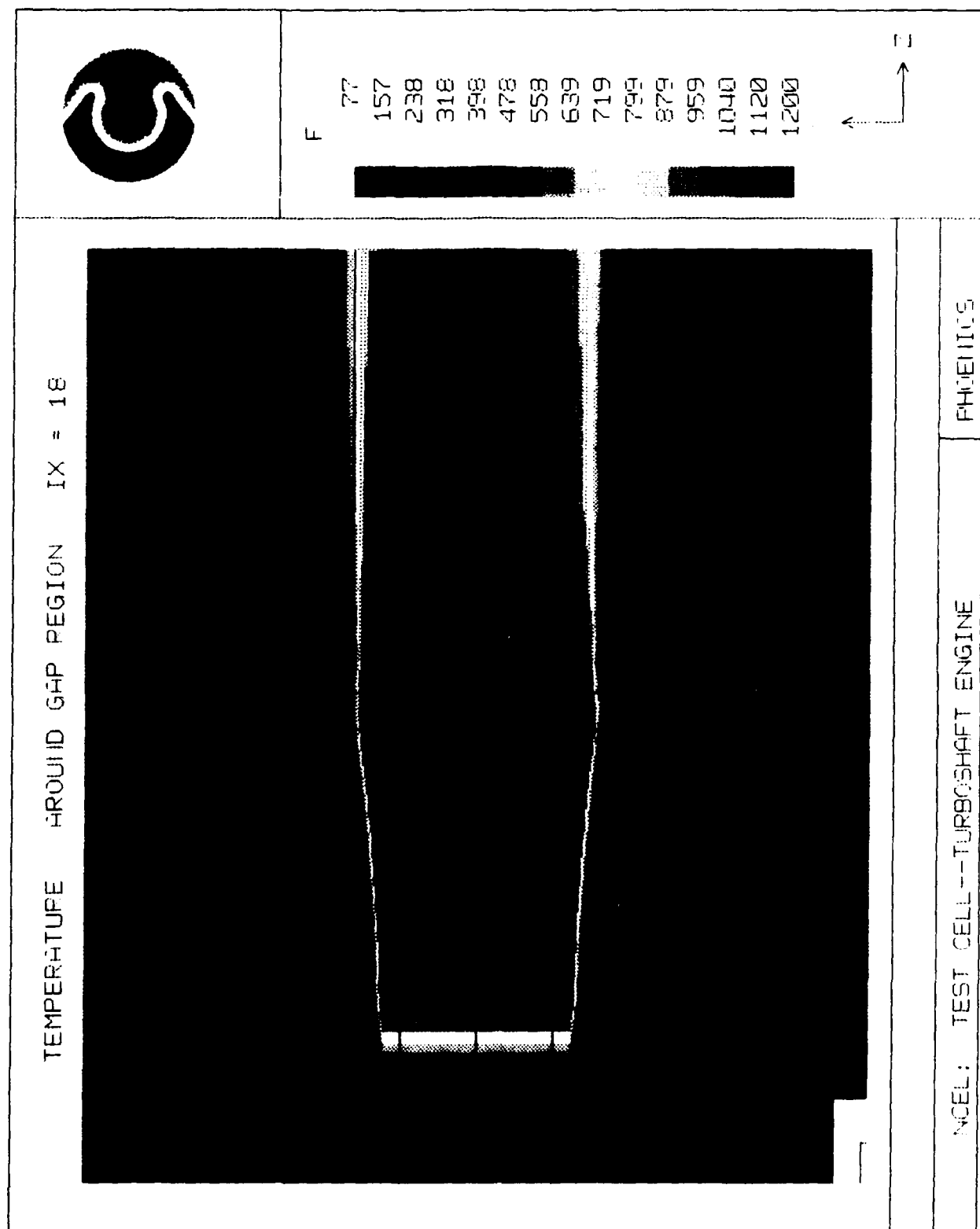
Figure 15. Temperature Around Gap Region

TEMPERATURE
AUGMENTER TUBE
Ix = 18

F
77
157
238
318
398
478
558
639
719
799
879
959
1040
1120
1200

N

NCEL: TEST CELL--TURBOSHAFT ENGINE   PHOENICS
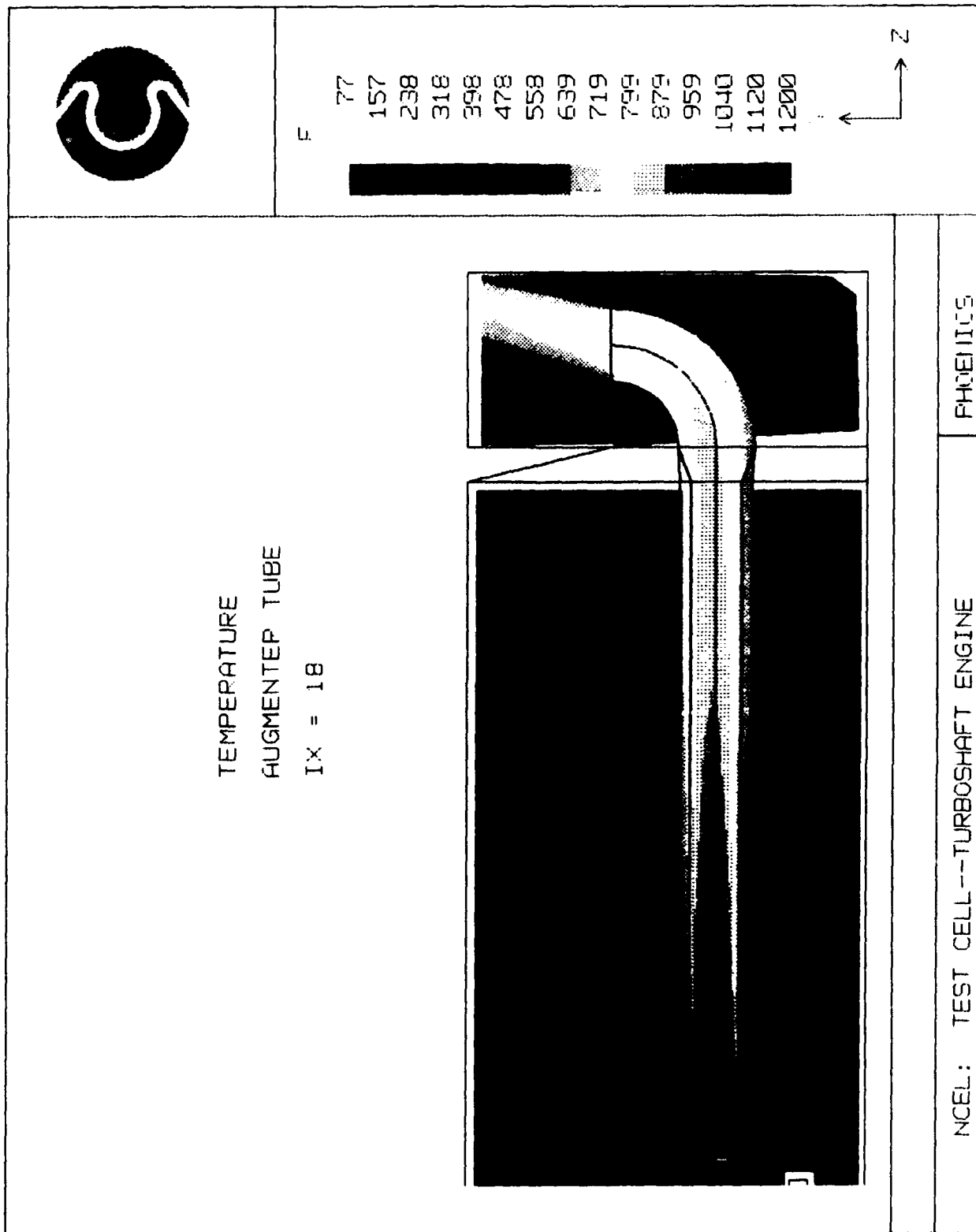
Figure16.   Temperature Augmenter Tube

37
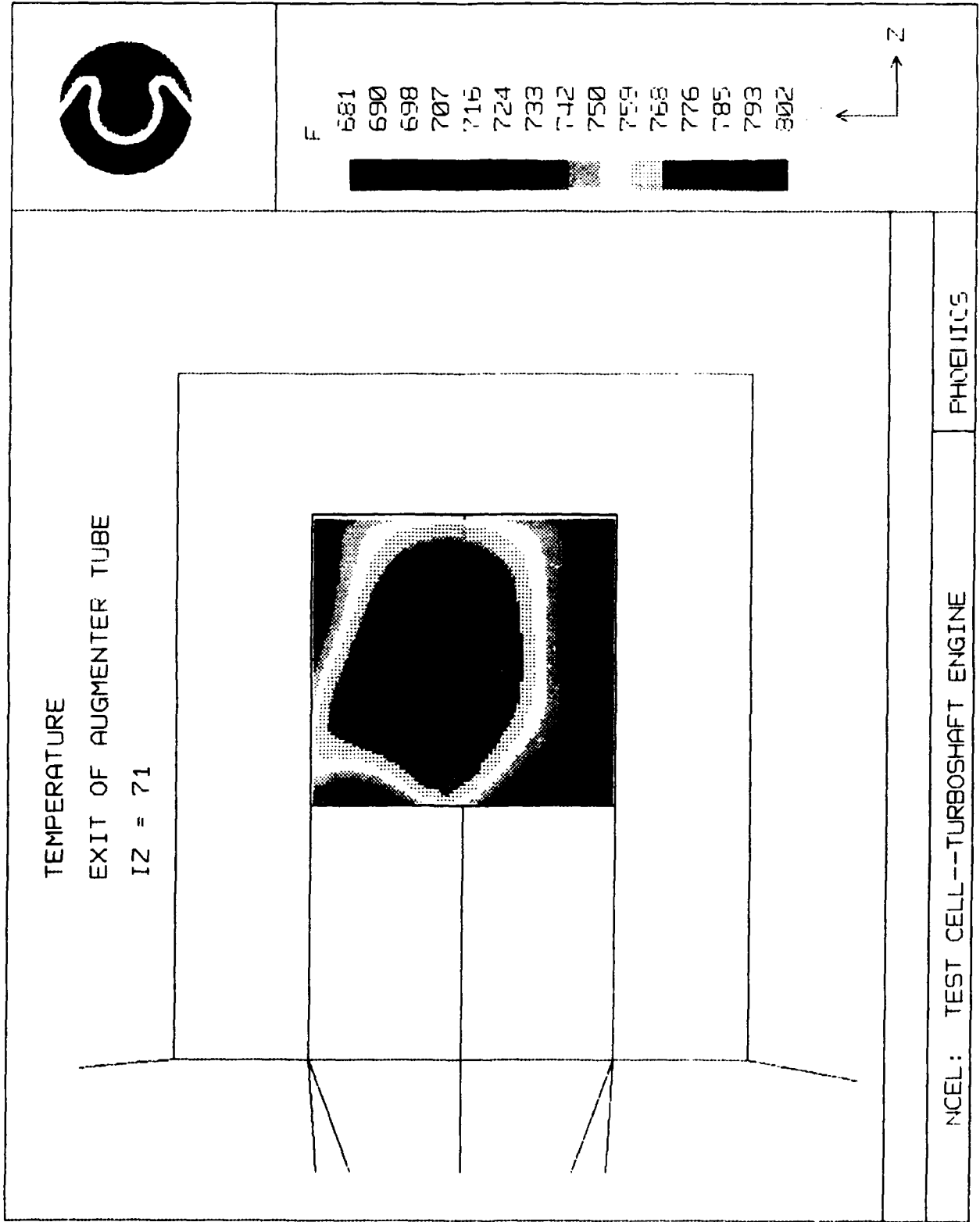
Figure 17. Temperature Exit of Augmenter Tube
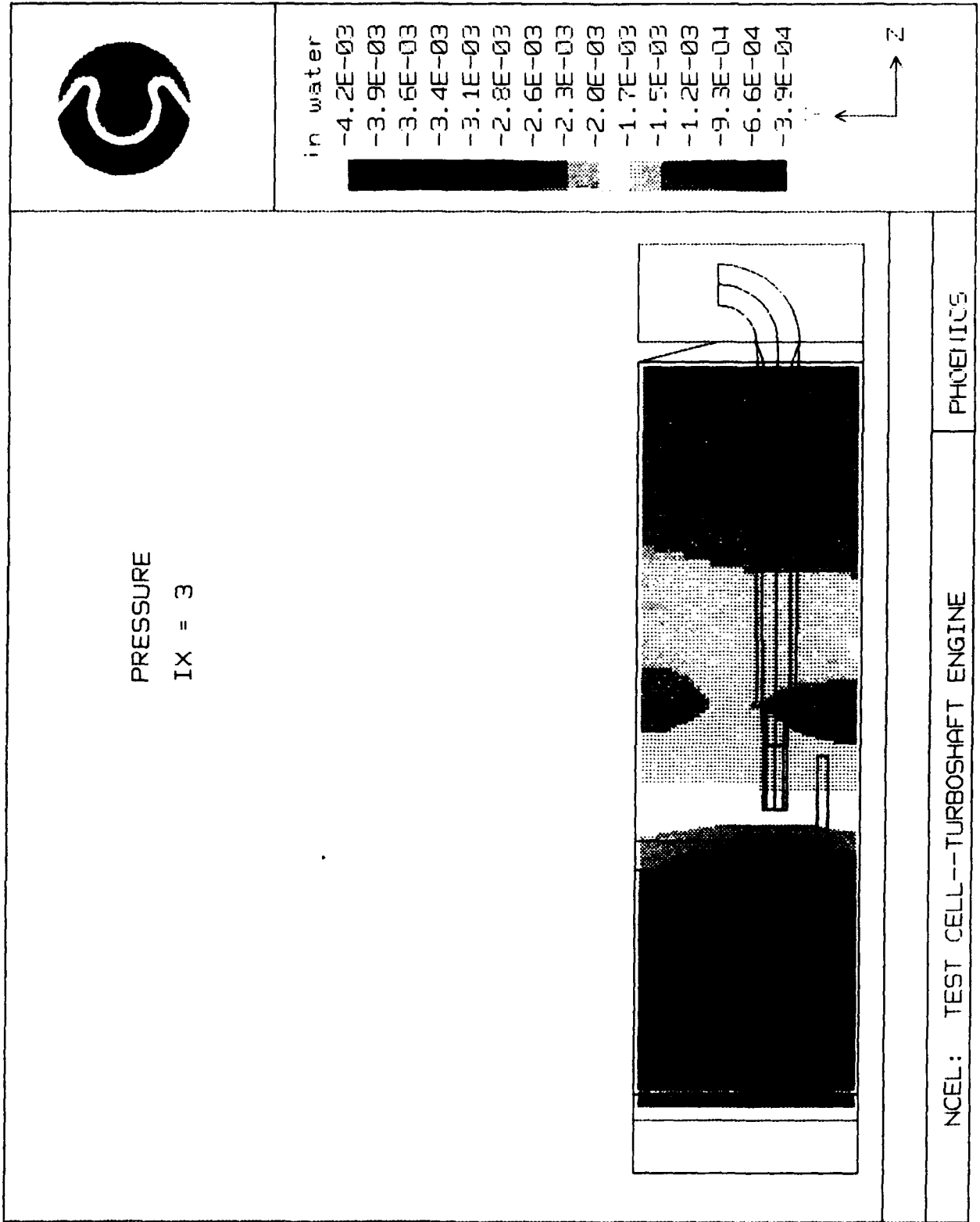
TEMPERATURE
EXIT OF CHIMNEY SECTION
IZ = 77

F
77
125
172
220
268
315
363
411
458
505
554
601
649
696
744

Z

NCEL: TEST CELL—TURBOSHAFT ENGINE

PHOENICS
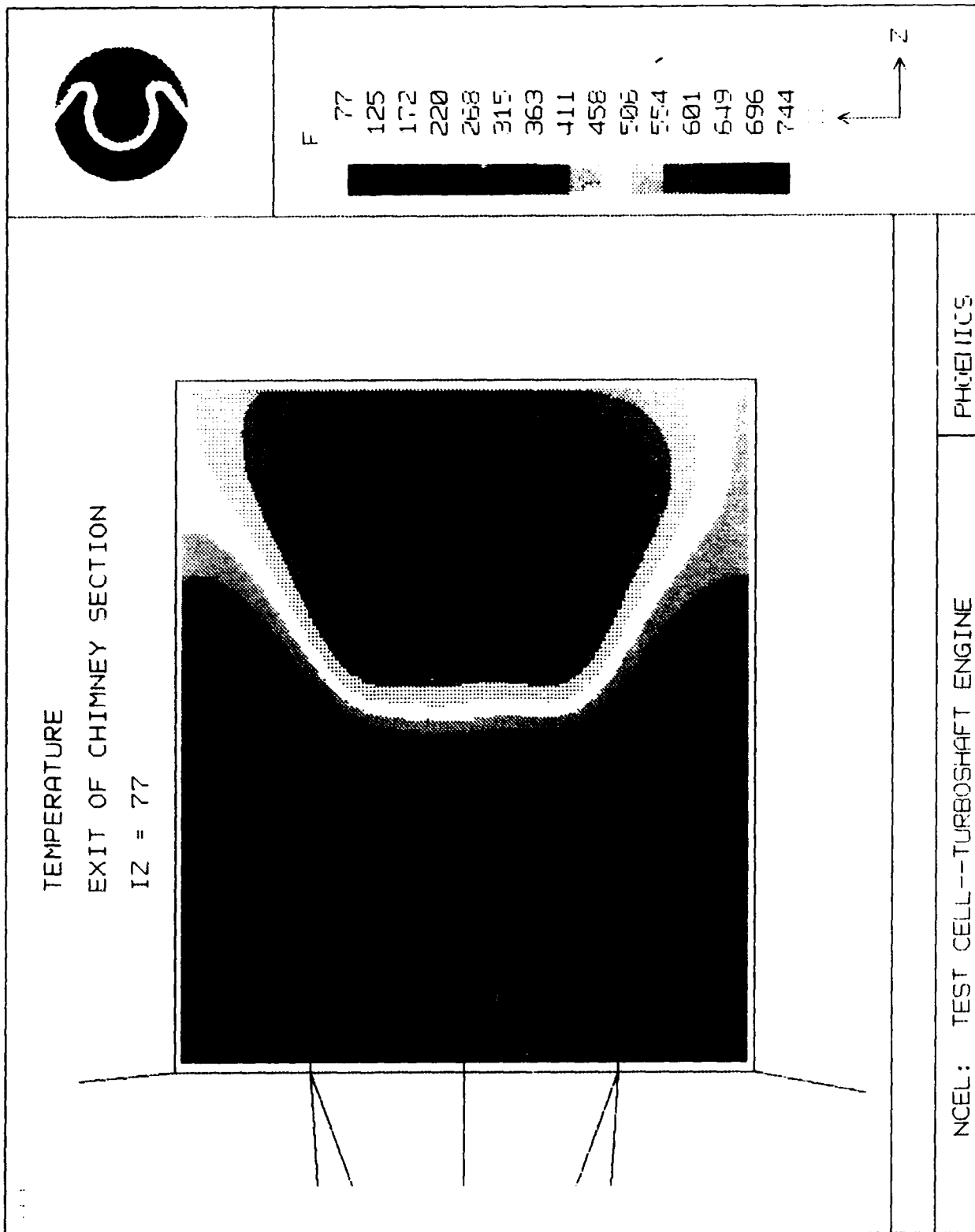
figure 18. Temperature Exit of Chimney Section
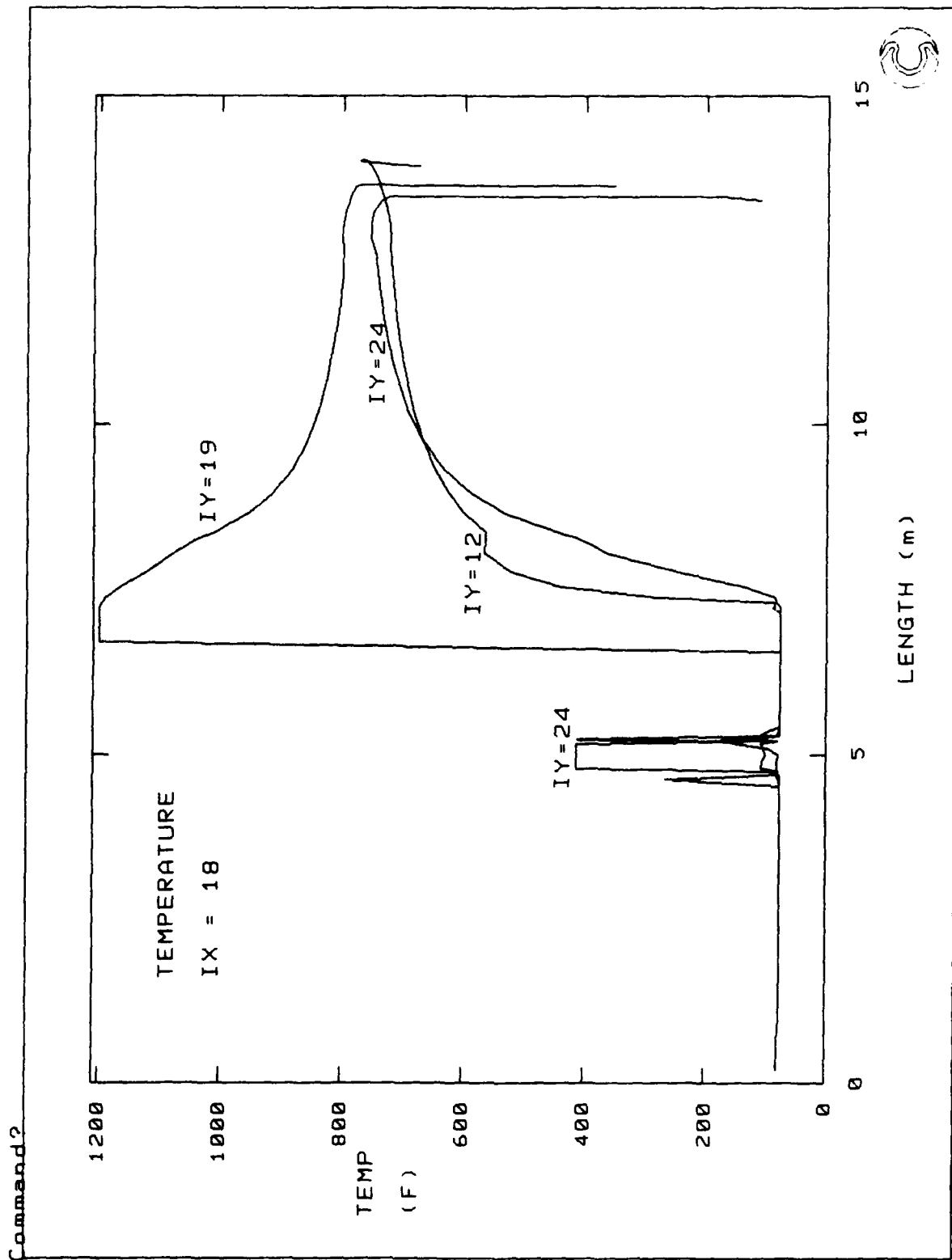
Figure 19.   Temperature vs. Length of Test Cell (at Three Vertical Locations)

PRESSURE

IX = 3

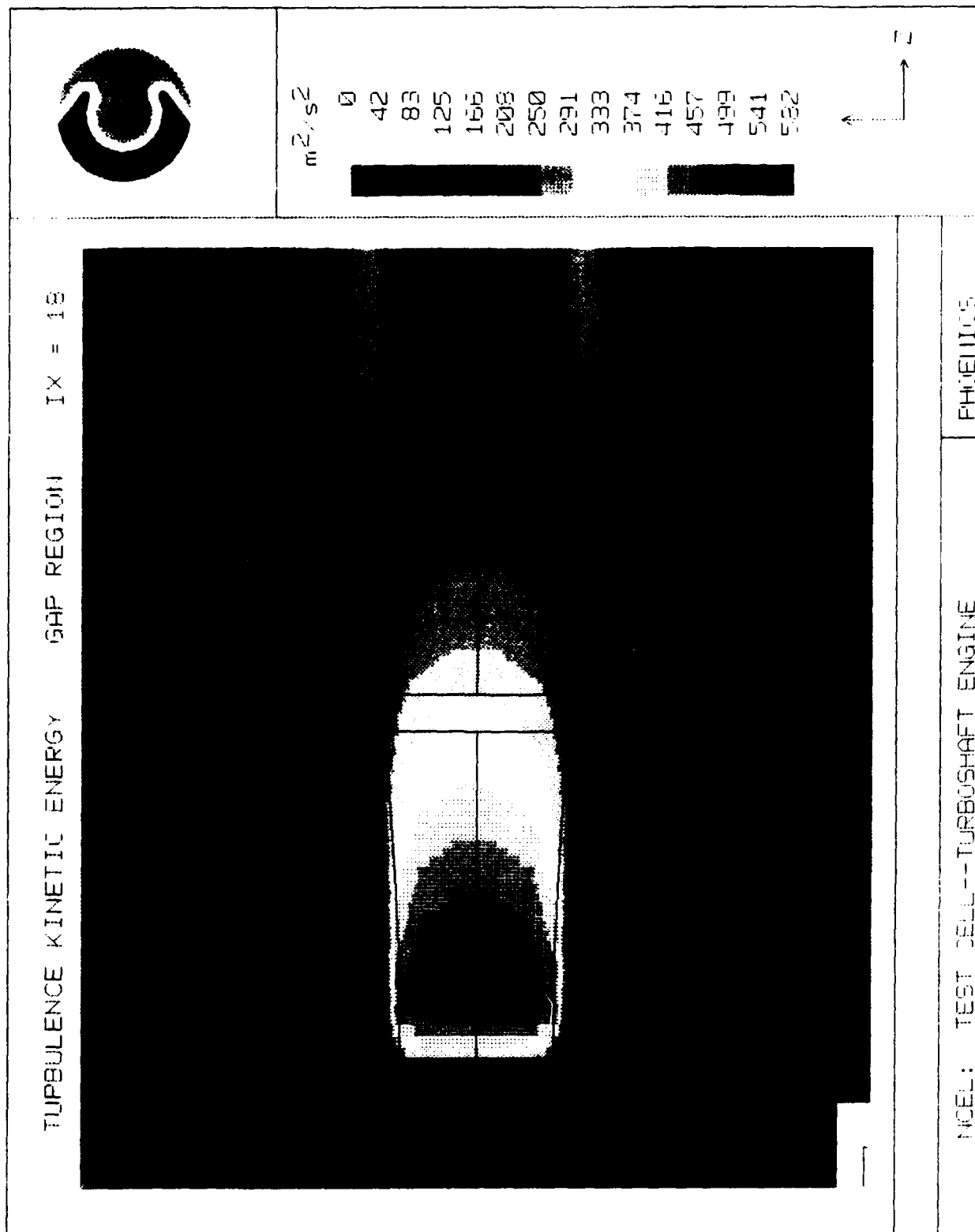in water

-4.2E-03
-3.9E-03
-3.6E-03
-3.4E-03
-3.1E-03
-2.8E-03
-2.6E-03
-2.3E-03
-2.0E-03
-1.7E-03
-1.5E-03
-1.2E-03
-9.3E-04
-6.6E-04
-3.9E-04

NCEL: TEST CELL—TURBOSHAFT ENGINE   PHOENICS

Figure 20.   Pressure

Figure 21.   Turbulence Kinetic Energy Gap Region
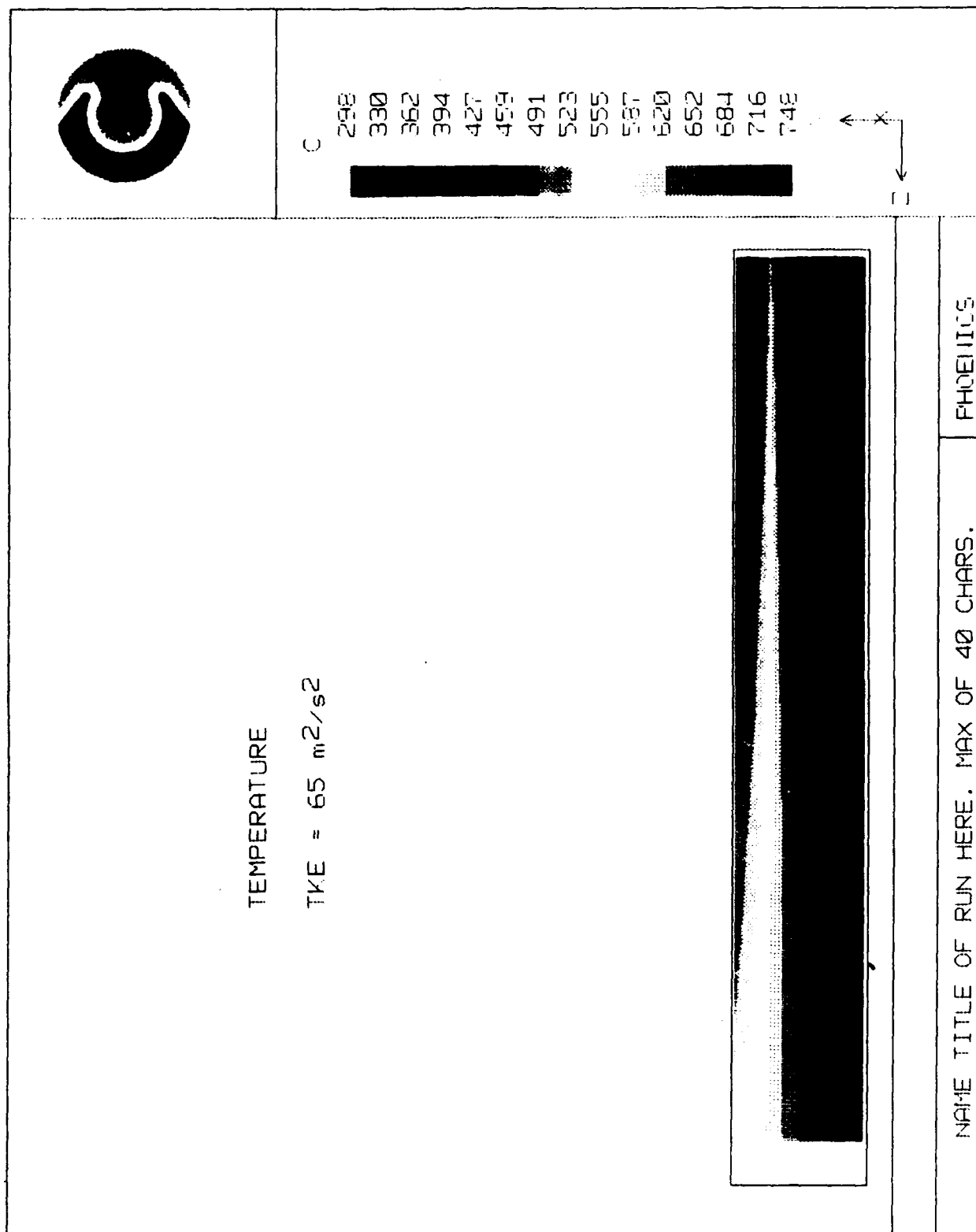
Figure 22. Temperature 2-D Model (TKE=65m^2/s^2)

43
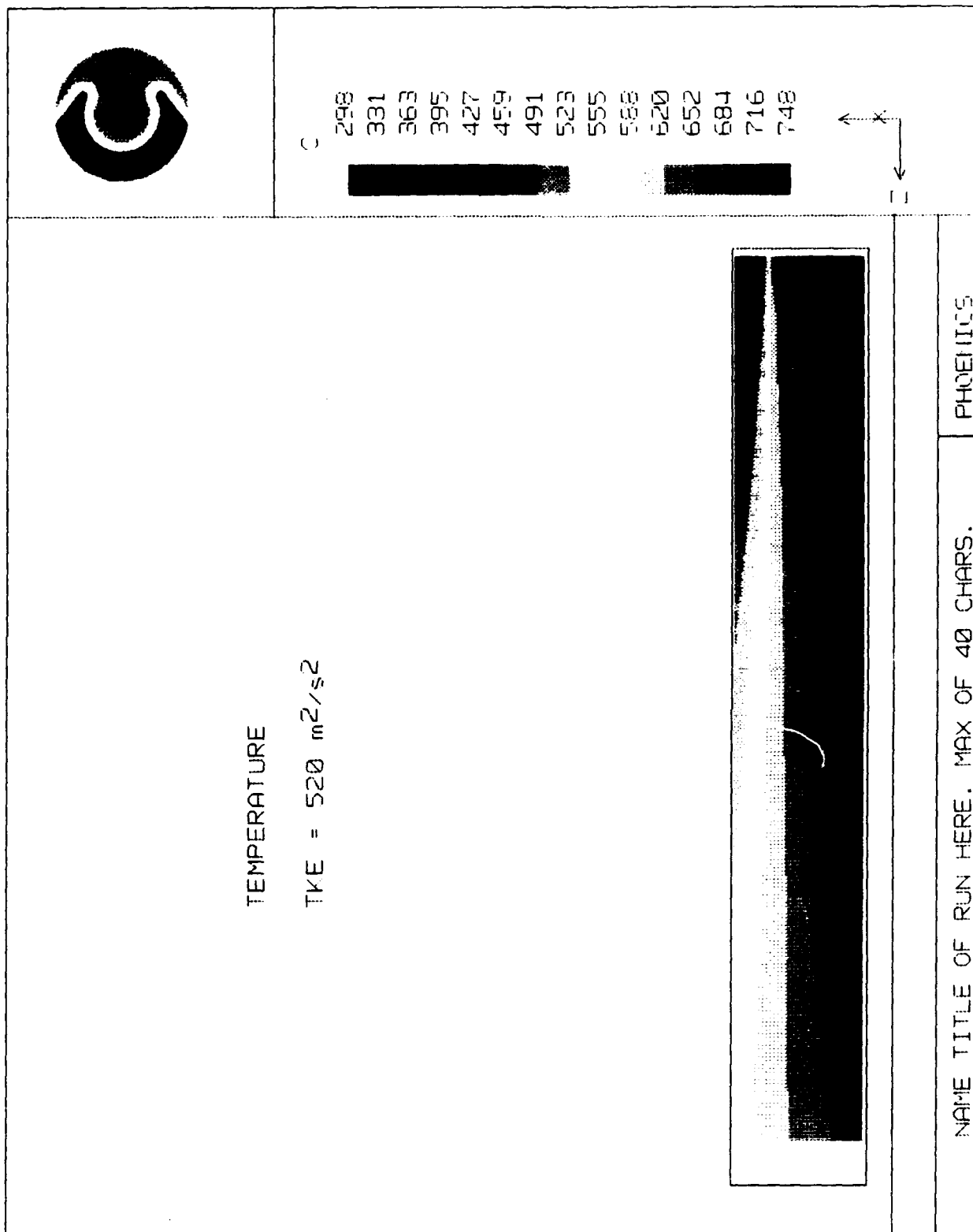
Figure 23. Temperature 2-D Model (TKE=520 m^2/s^2)
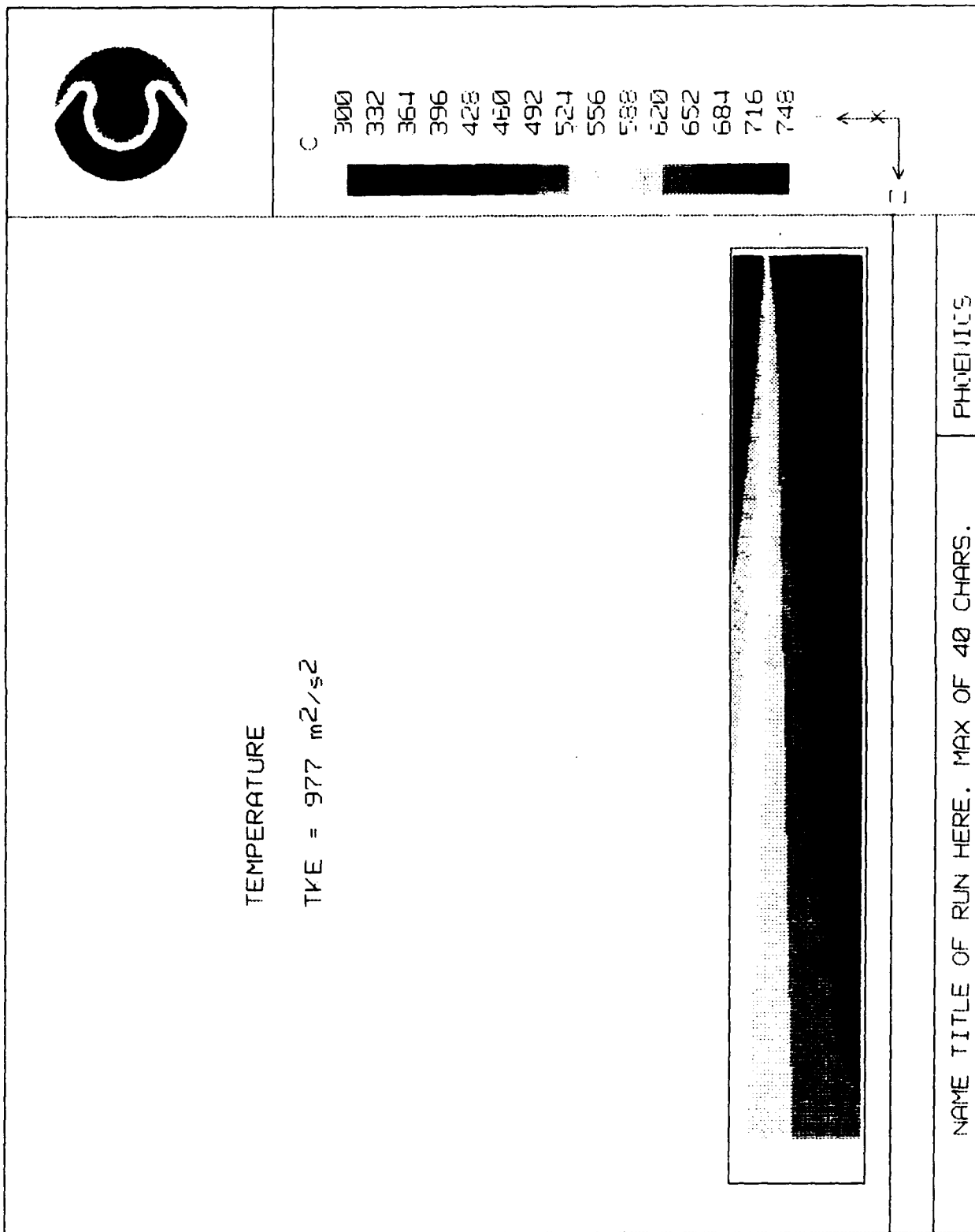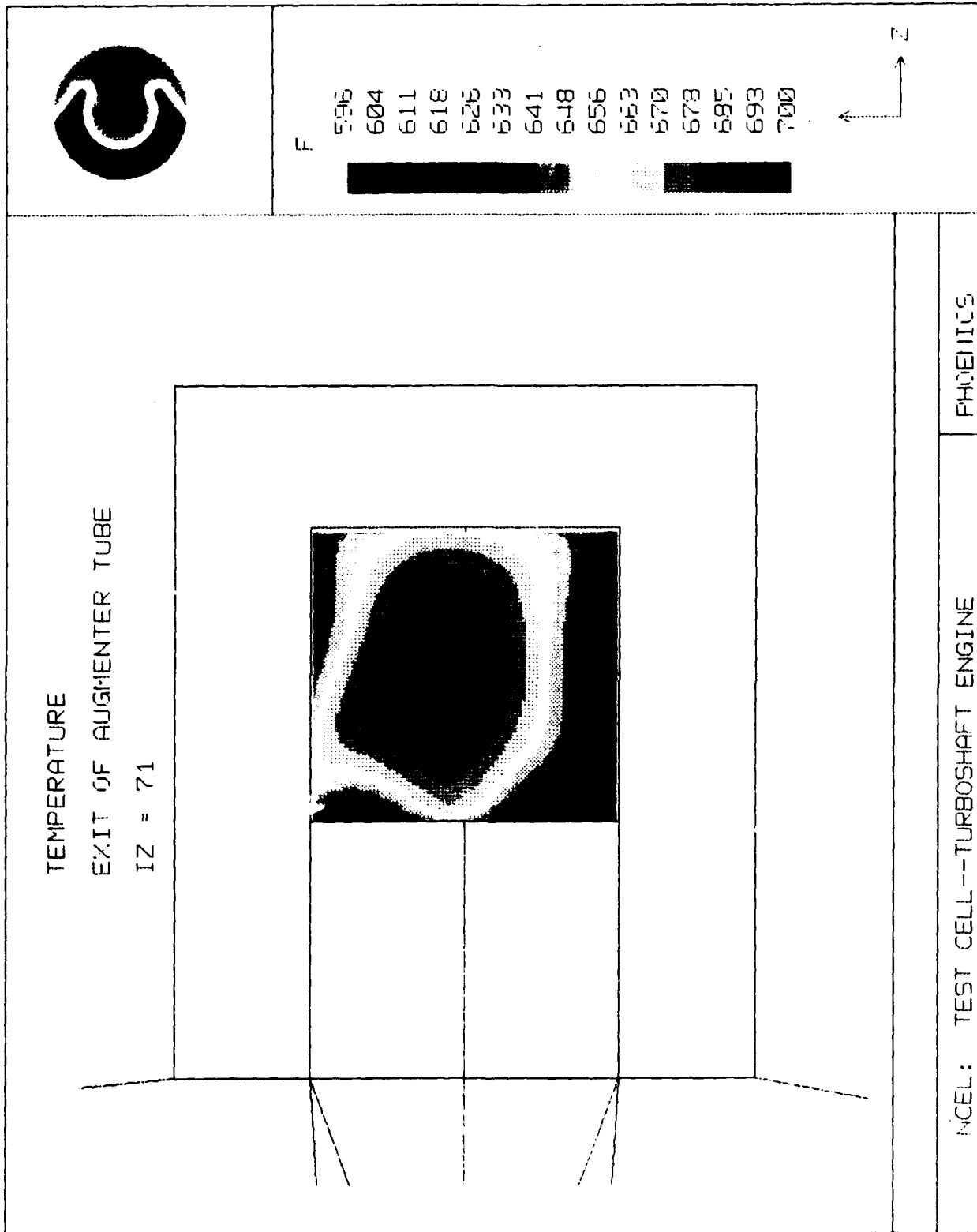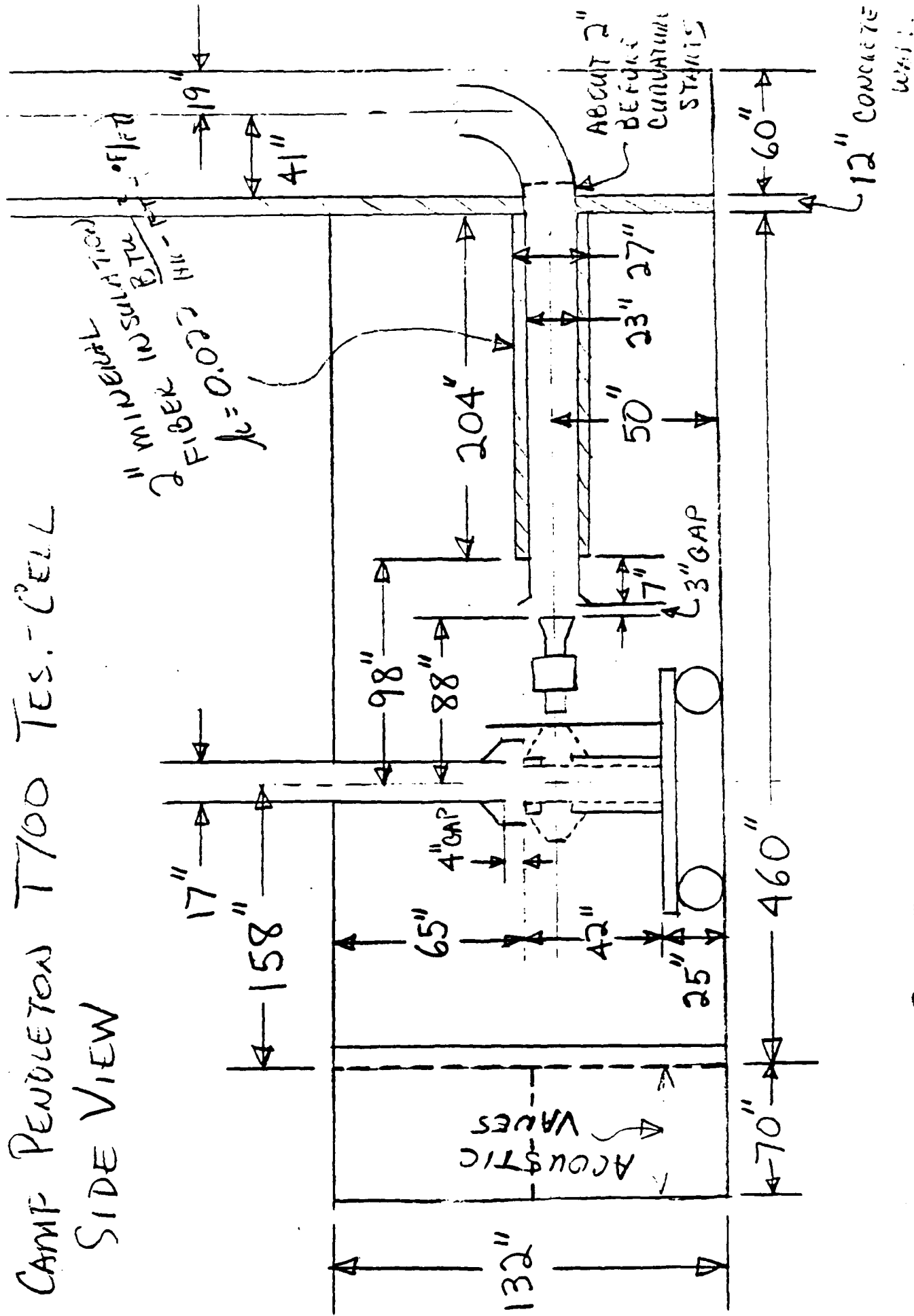
Figure 24. Temperature 2-D Model (TKE=977 m^2/s^2)

Figure 25. Temperature Exit of Augmenter Tube (Lower Engine Temperature)
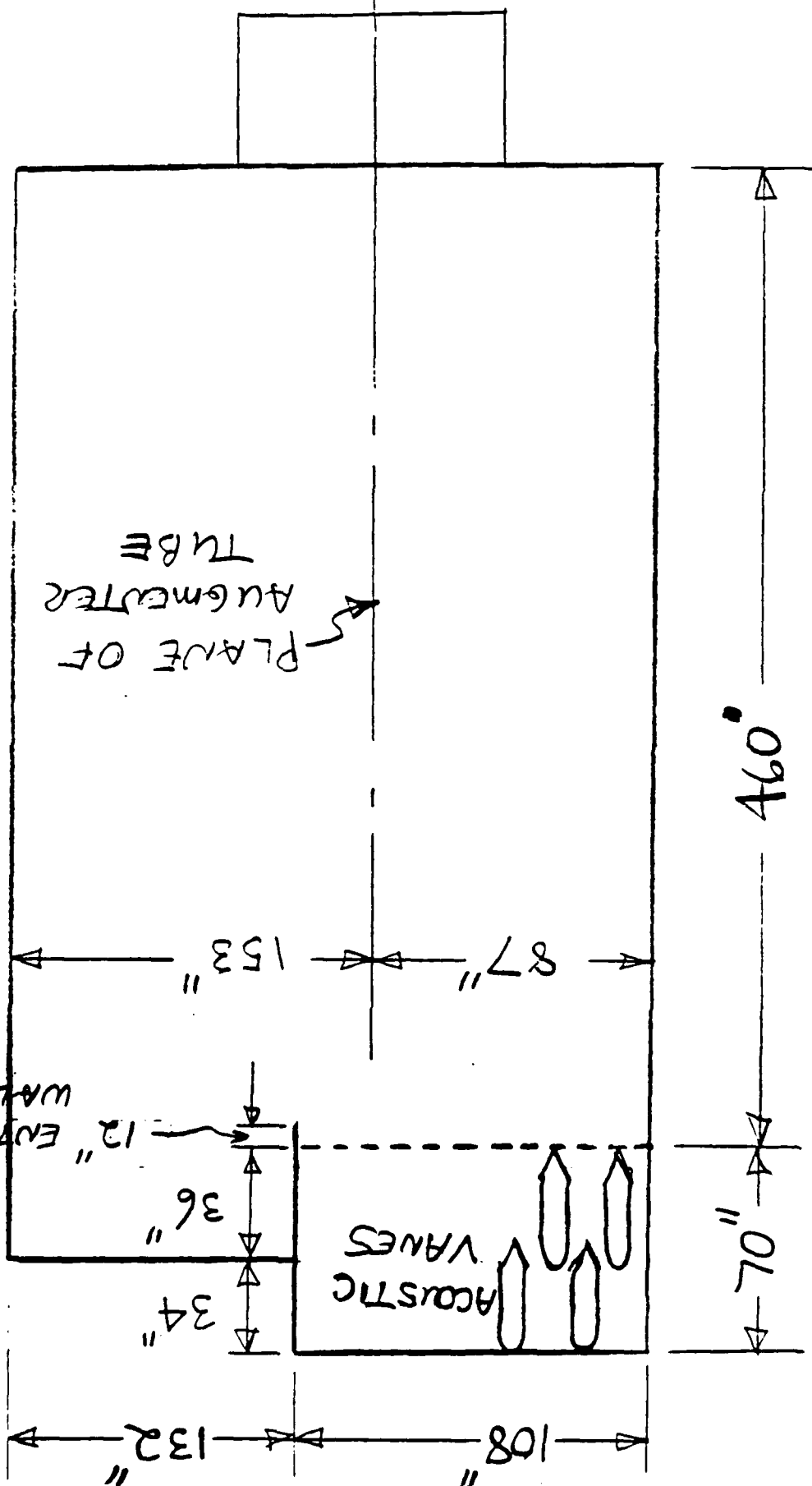
APPENDIX A

Camp Pendleton T/00 Tes.-Cell
Side View

2" Mineral Insulation
"Fiber Insulation"
$\lambda = 0.023 \frac{BTU}{Hr-Ft^2-°F/Ft}$

About 2" before curvature starts

12" Concrete wall

19"
41"
60"

204"
50"
23" 27"
7"
3" Gap

98"
88"

17"
158"

65"
42"
25"
4" Gap

460"

70"

132"

Acoustic Vanes

NOT TO SCALE
EVERYTHING IN INCHES

CAMP PENDLETON
T700 TEST CELL
TOP VIEW

PLANE OF
AUGMENTER
TUBE

960"

153"

87"

12" EXTENSION OF
WALL SURROUNDING
BAFFLES

36"

34"

ACOUSTIC
VANES

132"

108"

70"

6" THICK

ACOUSTIC BAFFLES EVENLY SPACED

6" THICK

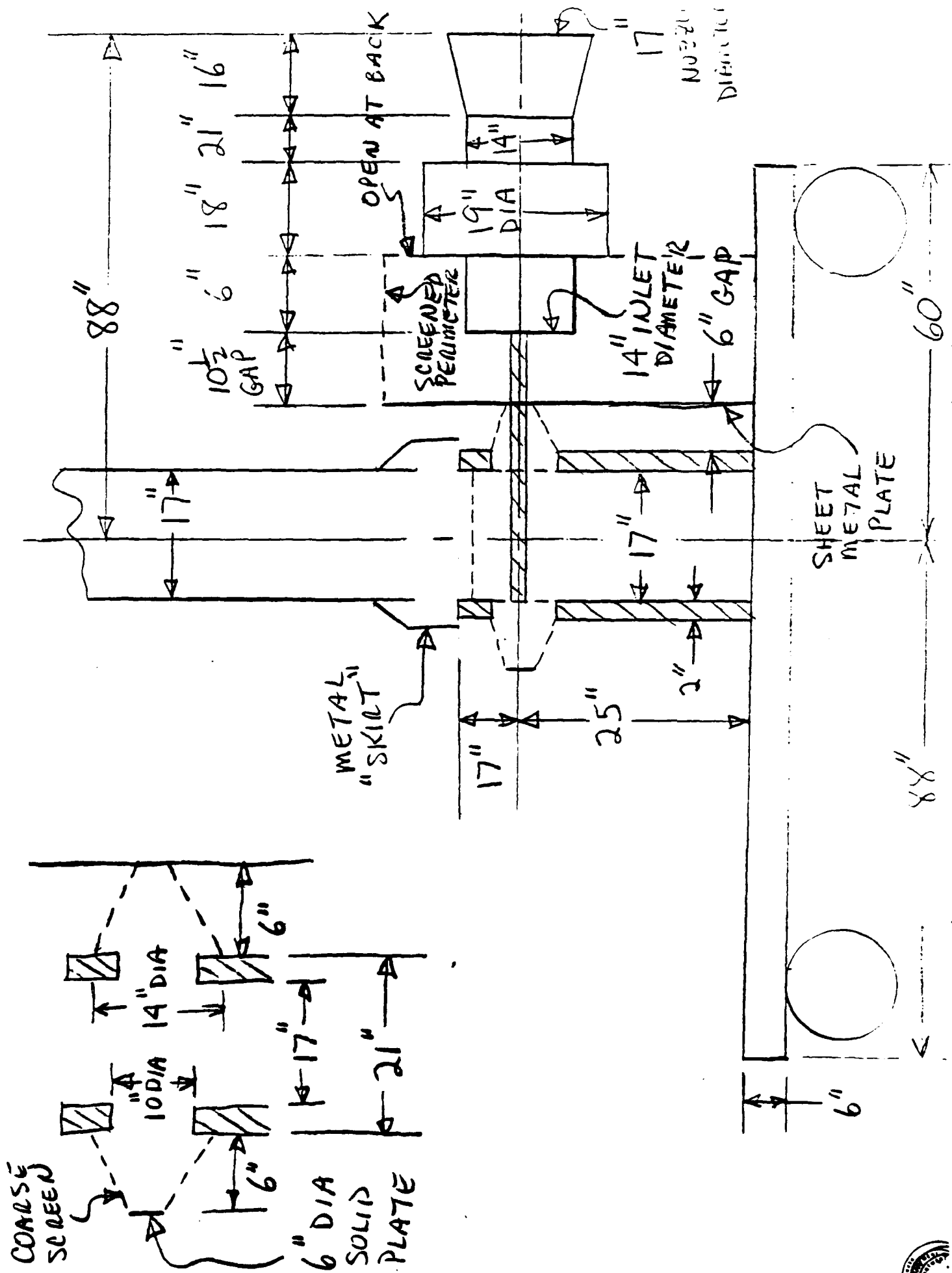← TOP VIEW →

6" THICK

60"

48"

100"

132"

31"

17"

158"
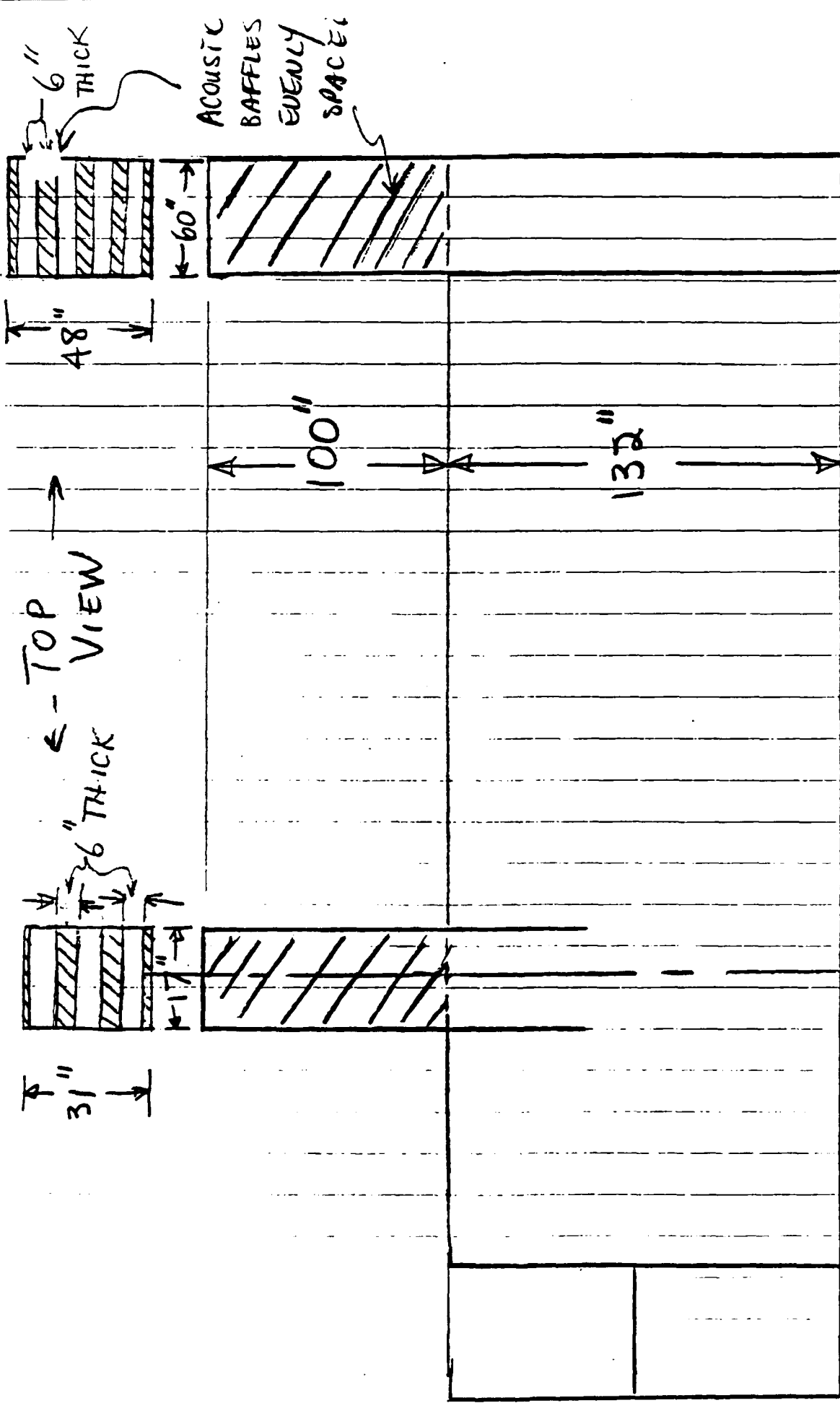
CAMP PENDLETON T700 CELL

SIDE VIEW

LOOKING TOWARD
ACOUSTIC VANES
FROM ENGINE

13 VANES

132"

13 VANES

108"
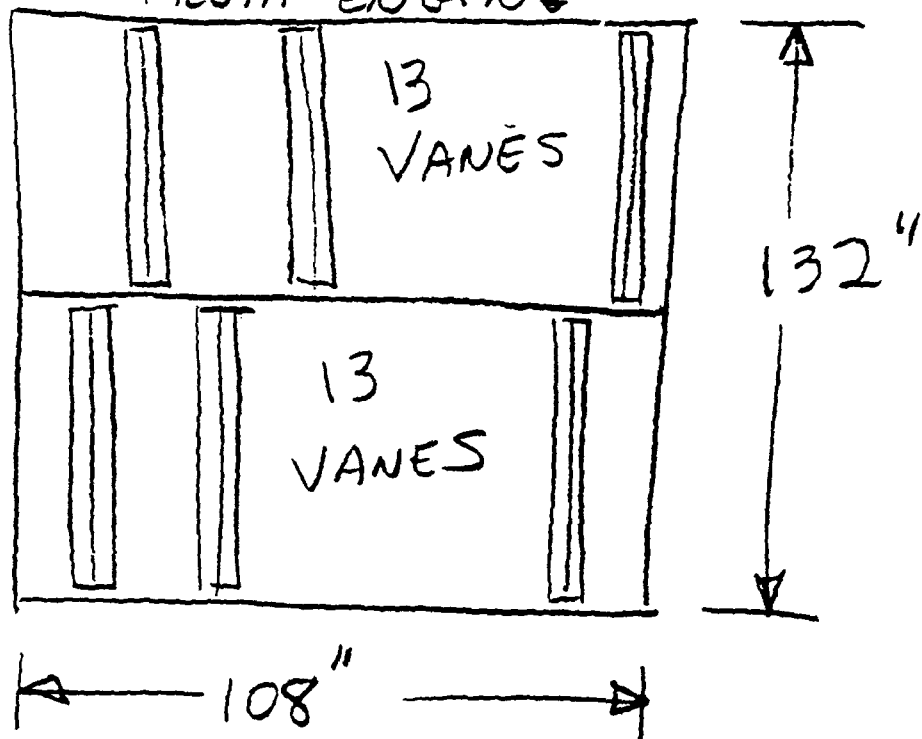
TOP VIEW, BOTTOM SET

70"

4"

47"

8"
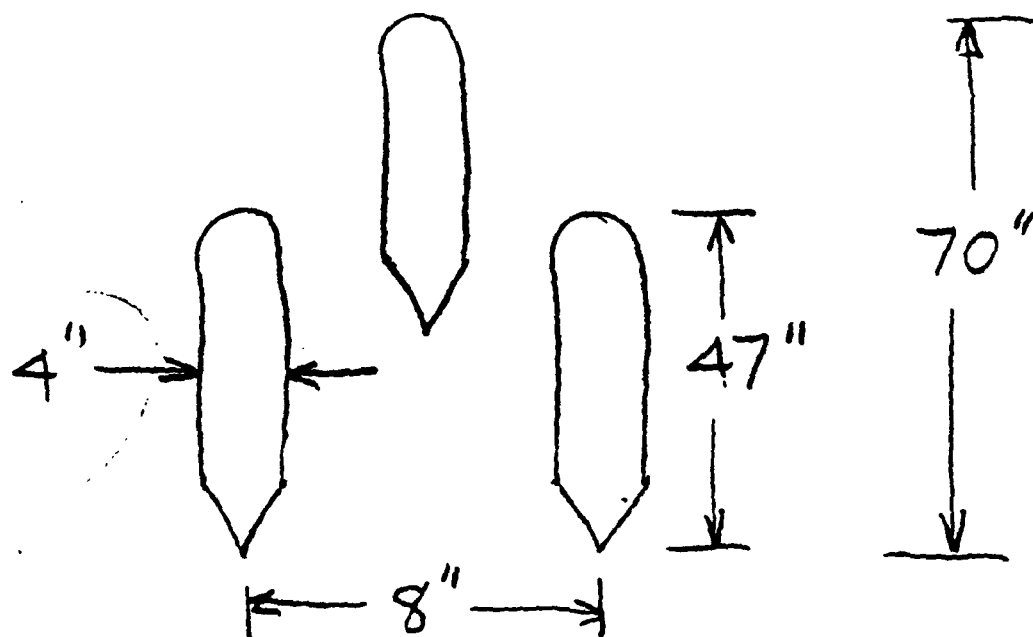
TYPE I SILENCER BAFFLE
REF BLUEPRINT S-18

DYNAMOMETER FRONT
LOOKING REARWARD

SHEET METAL PLATE

16"

10" DIAMETER INLET TO DYNA.

16"

17"

36"

25"

APPROX 2" WALL

31"

SIDES SOLI

FLOOR ON TOP OF "CART"

25"

BOTTOM OPEN

48"
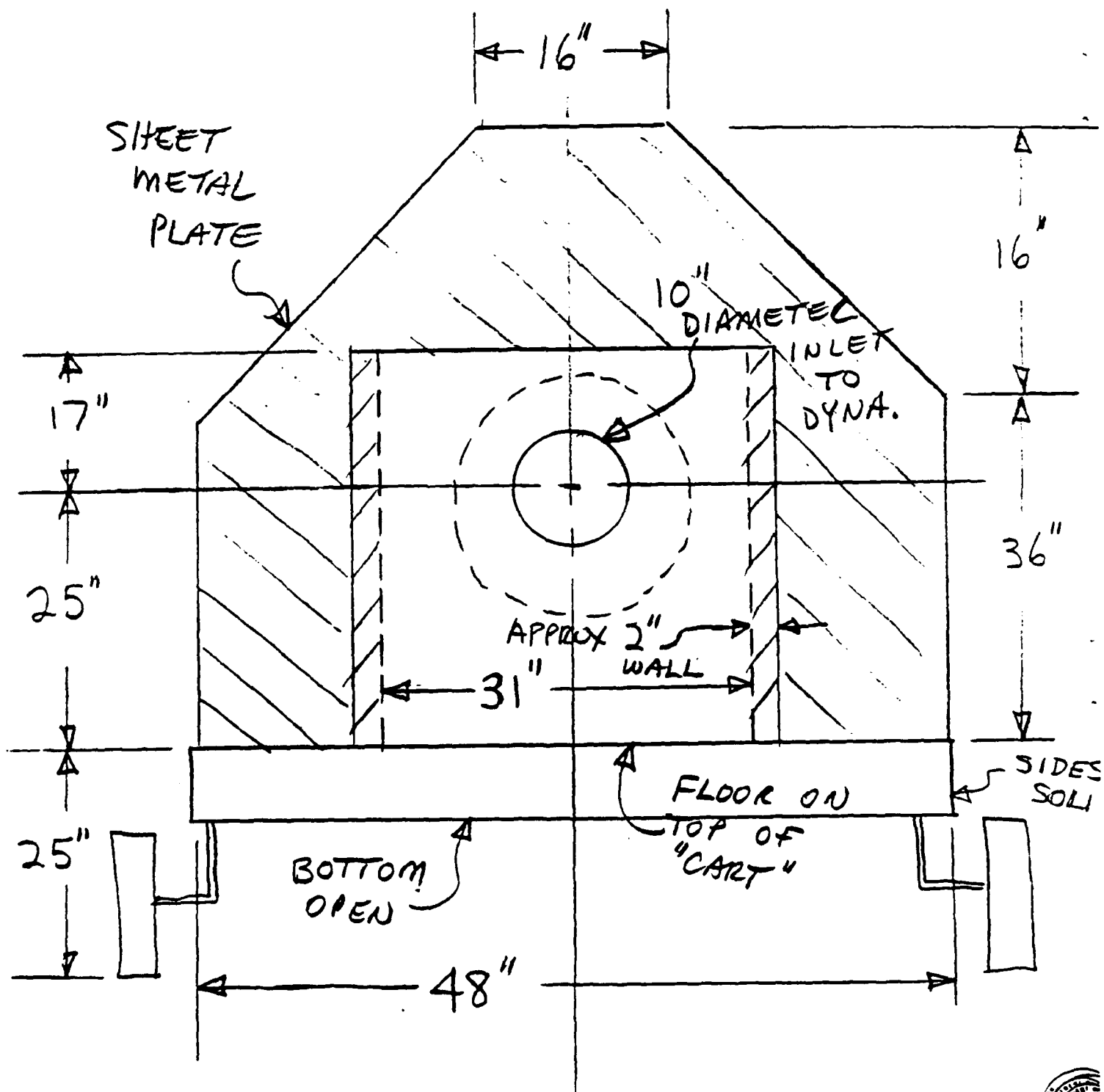
CAMP PENDLETON T700 TEST CELL DYNAMOMETER EXHAUST DUCT

SIDE VIEW

FRONT VIEW

61"

17"

36"

65"

METAL "SKIRT"

4" GAP

31"

39"

3½"

4½"

T700
CHIMNEY
SIDE VIEW

$27\frac{1}{2}$" $25\frac{1}{2}$" 7"

SQUARE

23"

ROUND

TOP 0.
OUTER
SURF. i
TOP 0,
TUBE

2"

53"

"

60"

12"

FRONT
VIEW

48"

$25\frac{1}{2}$"
CENTERED

23" DIAMETER

2" MINERAL FIBRE INSULATION

$$k \sim 0.022 \frac{Btu}{HR - FT^2 - (^\circ F)}$$

$1\frac{1}{2}"$

$2\frac{1}{2}"$

CAMP PENDLETON
T700 AUGMENTER
TUBE
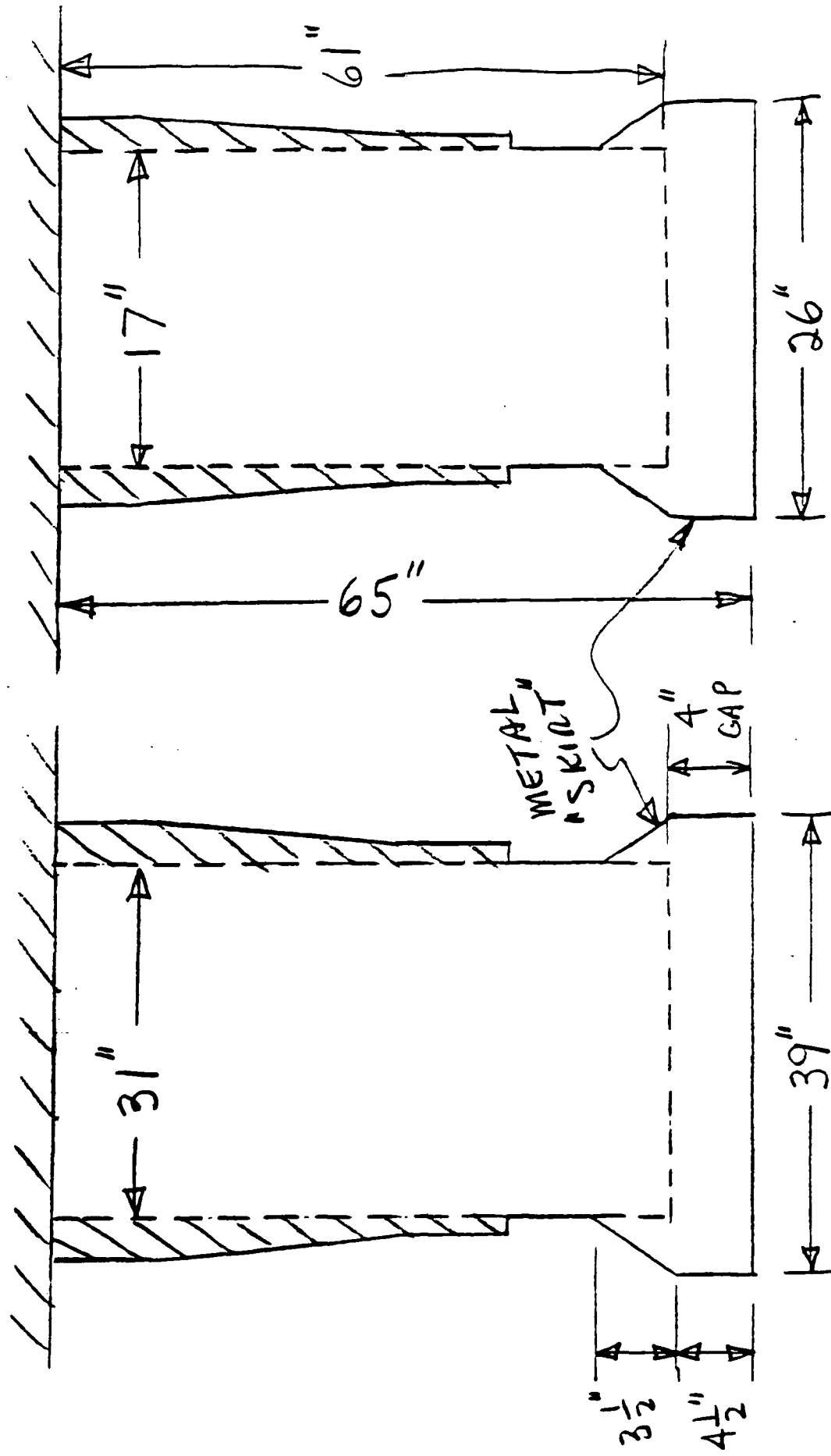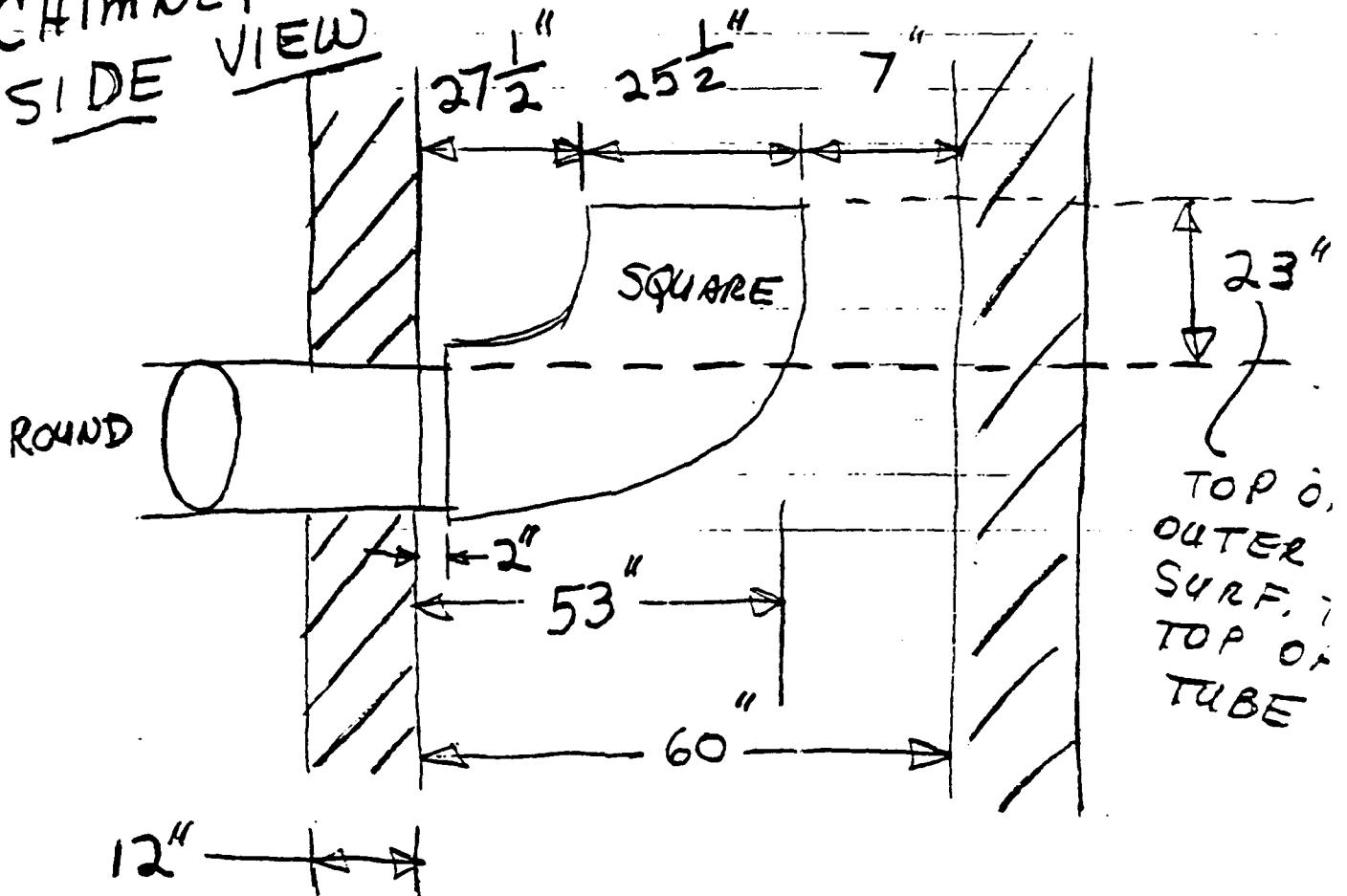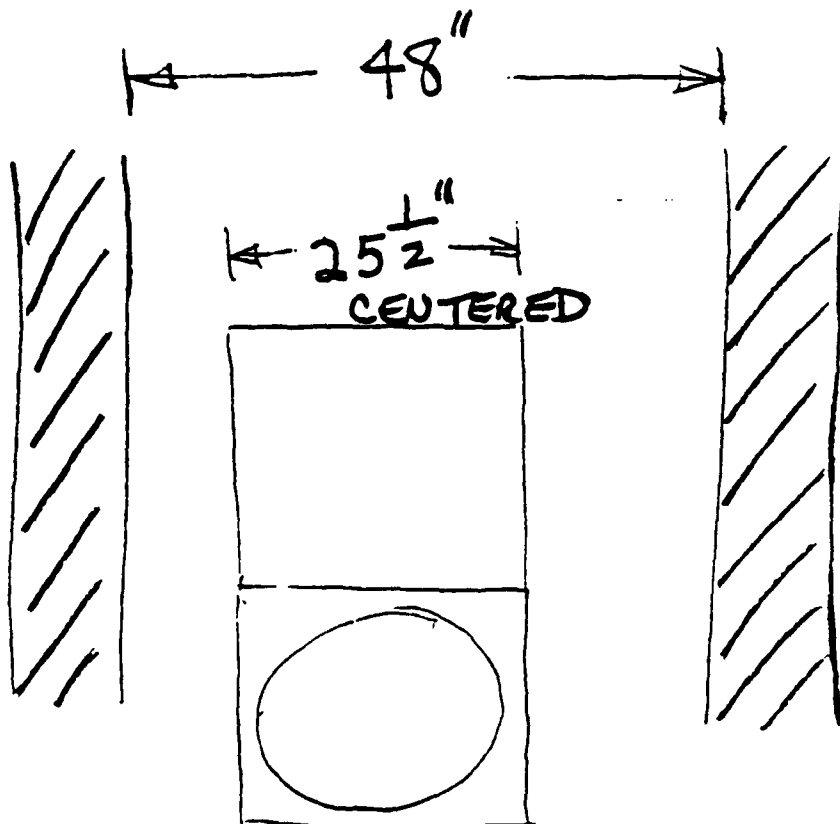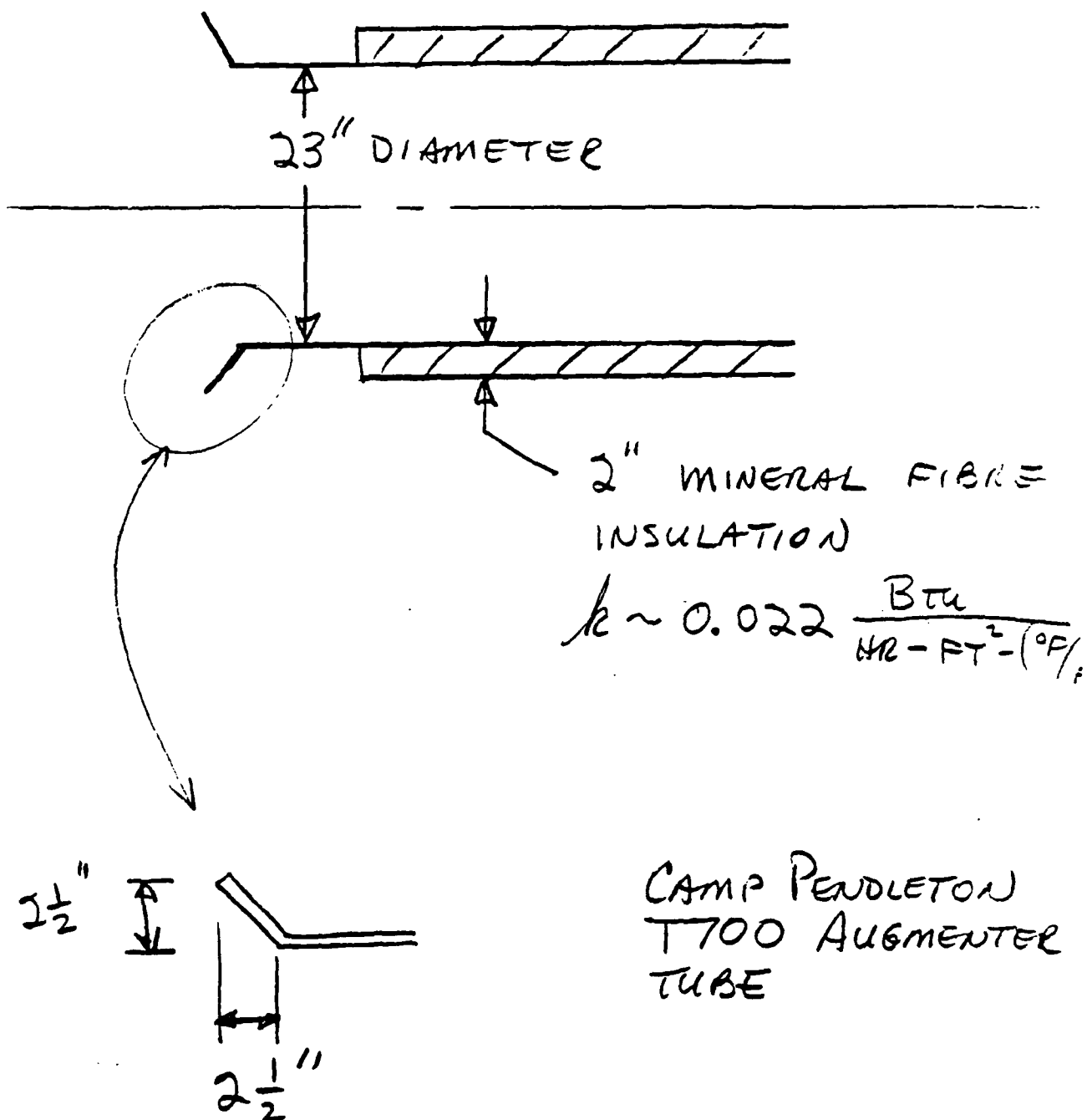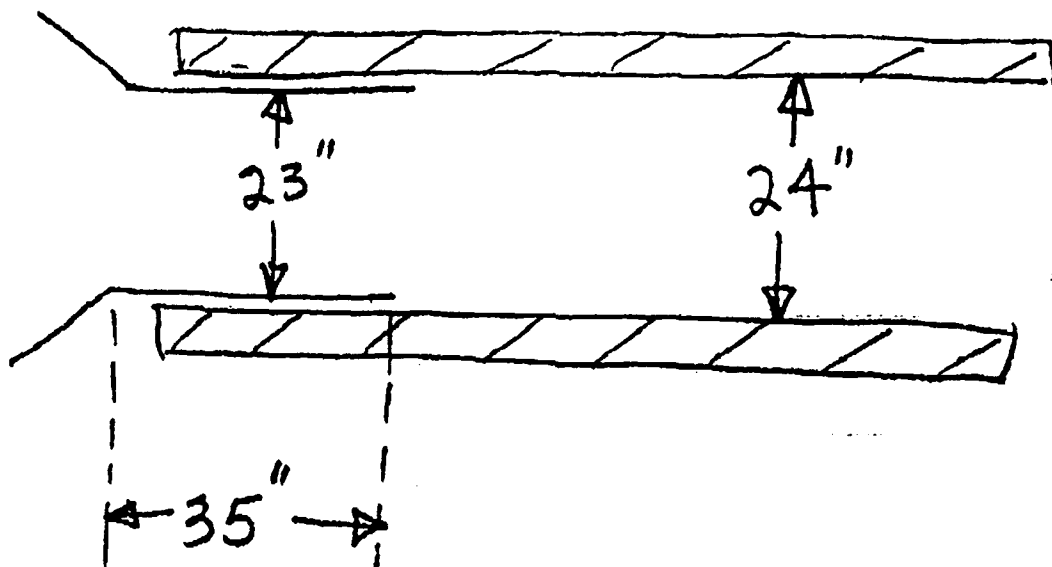
$$\text{PUMPING RATIO} \equiv \frac{\text{SECONDARY FLOW}}{\text{ENGINE FLOW}}$$

$$= \frac{28.3 - 11.2}{11.2} = 1.53$$

ETC. FOR DYNAMOMETER

CELL DEPRESSION IS A NEGATIVE GAUGE
PRESSURE MEASURED INSIDE THE TEST BAY.

INSTALLATION OF T700 in T-16 TEST CELL

LONG TEST TAILPIPE

Engine C_L Concentric with Augmenter Tube C_L.

Figure 4. T700 Installation in T-16 Test Cell with Long Test Tailpipe and Engine Centered.

DISTRIBUTION QUESTIONNAIRE
The Naval Civil Engineering Laboratory is revising its primary distribution lists.

SUBJECT CATEGORIES

1 SHORE FACILITIES
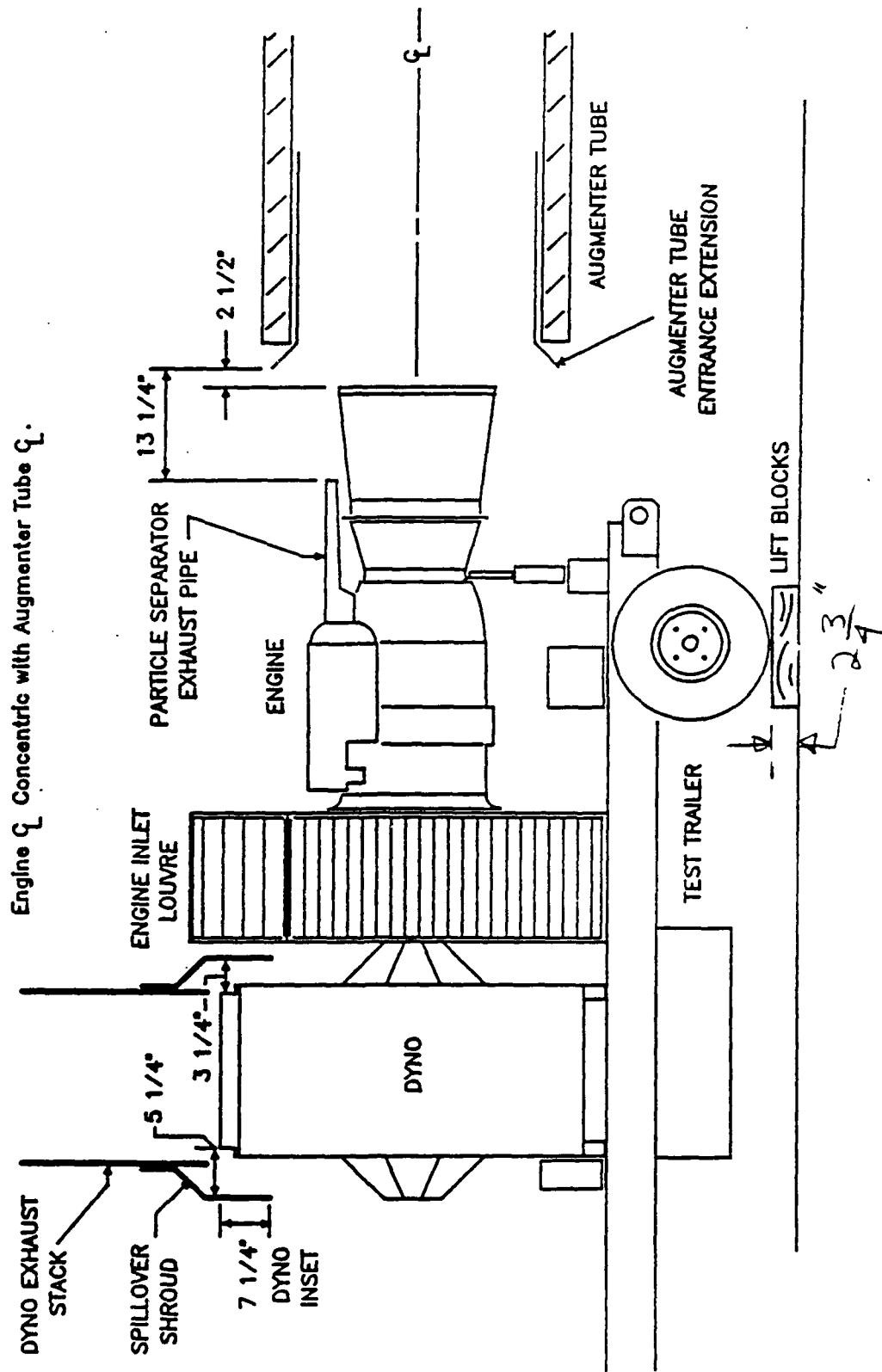1A Construction methods and materials (including corrosion control, coatings)
1B Waterfront structures (maintenance/deterioration control)
1C Utilities (including power conditioning)
1D Explosives safety
1E Aviation Engineering Test Facilities
1F Fire prevention and control
1G Antenna technology
1H Structural analysis and design (including numerical and computer techniques)
1J Protective construction (including hardened shelters, shock and vibration studies)
1K Soil/rock mechanics
1L Airfields and pavements
1M Physical security
2 ADVANCED BASE AND AMPHIBIOUS FACILITIES
2A Base facilities (including shelters, power generation, water supplies)
2B Expedient roads/airfields/bridges
2C Over-the-beach operations (including breakwaters, wave forces)
2D POL storage, transfer, and distribution
2E Polar engineering
3 ENERGY/POWER GENERATION
3A Thermal conservation (thermal engineering of buildings, HVAC systems, energy loss measurement, power generation)
3B Controls and electrical conservation (electrical systems, energy monitoring and control systems)
3C Fuel flexibility (liquid fuels, coal utilization, energy from solid waste)

3D Alternate energy source (geothermal power, photovoltaic power systems, solar systems, wind systems, energy storage systems)
3E Site data and systems integration (energy resource data, integrating energy systems)
3F EMCS design
4 ENVIRONMENTAL PROTECTION
4A Solid waste management
4B Hazardous/toxic materials management
4C Waterwaste management and sanitary engineering
4D Oil pollution removal and recovery
4E Air pollution
4F Noise abatement
5 OCEAN ENGINEERING
5A Seafloor soils and foundations
5B Seafloor construction systems and operations (including diver and manipulator tools)
5C Undersea structures and materials
5D Anchors and moorings
5E Undersea power systems, electromechanical cables, and connectors
5F Pressure vessel facilities
5G Physical environment (including site surveying)
5H Ocean-based concrete structures
5J Hyperbaric chambers
5K Undersea cable dynamics
ARMY FEAP
BDG Shore Facilities
NRG Energy
ENV Environmental/Natural Responses
MGT Management
PRR Pavements/Railroads

TYPES OF DOCUMENTS

D – Techdata Sheets; R – Technical Reports and Technical Notes; G – NCEL Guides and Abstracts; I – Index to TDS; U – User Guides; ☐ None - remove my name

Old Address:

_____

_____

_____

_____

Telephone No.: _____

New Address:

_____

_____

_____

_____

Telephone No.: _____

INSTRUCTIONS

The Naval Civil Engineering Laboratory has revised its primary distribution lists. To help us verify our records and update our data base, please do the following:

- Add - circle number on list

- Remove my name from all your lists - check box on list.

- Change my address - line out incorrect line and write in correction (DO NOT REMOVE LABEL).

- Number of copies should be entered after the title of the subject categories you select.

- Are we sending you the correct type of document? If not, circle the type(s) of document(s) you want to receive listed on the back of this card.

Fold on line, staple, and drop in mail.

DEPARTMENT OF THE NAVY
Naval Civil Engineering Laboratory
560 Laboratory Drive
Port Hueneme CA 93043-4328

Official Business
Penalty for Private Use, $300

BUSINESS REPLY CARD
FIRST CLASS   PERMIT NO. 12503   WASH D.C.

POSTAGE WILL BE PAID BY ADDRESSEE

**COMMANDING OFFICER
CODE L34
560 LABORATORY DRIVE
NAVAL CIVIL ENGINEERING LABORATORY
PORT HUENEME CA 93043-4328**

NCEL DOCUMENT EVALUATION

You are number one with us; how do we rate with you?

We at NCEL want to provide you our customer the best possible reports but we need your help. Therefore, I ask you to please take the time from your busy schedule to fill out this questionnaire. Your response will assist us in providing the best reports possible for our users. I wish to thank you in advance for your assistance. I assure you that the information you provide will help us to be more responsive to your future needs.

R. N. Storer

R. N. STORER, Ph.D, P.E.
Technical Director

DOCUMENT NO. _____ TITLE OF DOCUMENT: _____

_____

Date: _____ Respondent Organization : _____

Name: _____ Activity Code: _____
Phone: _____ Grade/Rank: _____

Category (*please check*):

    Sponsor _____   User _____   Proponent _____   Other (*Specify*) _____

Please answer on your behalf only; not on your organization's. Please check (*use an X*) only the block that most closely describes your attitude or feeling toward that statement:

    SA   Strongly Agree   **A** Agree   **O**   Neutral   **D**   Disagree   **SD**   Strongly Disagree

---

                                        SA A N D SD   **SA A N D SD**

1. The technical quality of the report   ( ) ( ) ( ) ( ) ( )   6. The conclusions and recommenda-   ( ) ( ) ( ) ( ) ( )
   is comparable to most of my other   tions are clear and directly sup-
   sources of technical information.   ported by the contents of the
                                                      report.

2. The report will make significant   ( ) ( ) ( ) ( ) ( )
   improvements in the cost and or   7. The graphics, tables, and photo-   ( ) ( ) ( ) ( ) ( )
   performance of my operation.   graphs are well done.

3. The report acknowledges related   ( ) ( ) ( ) ( ) ( )
   work accomplished by others.

                                                  Do you wish to continue getting   ☐   ☐
4. The report is well formatted.   ( ) ( ) ( ) ( ) ( )   NCEL reports?   **YES**   **NO**

5. The report is clearly written.   ( ) ( ) ( ) ( ) ( )   Please add any comments (e.g., in what ways can we
                                                       improve the quality of our reports?) on the back of this
                                                       form.

Comments:

Fold on line, staple, and drop in mail.

BUSINESS REPLY CARD
FIRST CLASS   PERMIT NO. 12503   WASH D.C.

POSTAGE WILL BE PAID BY ADDRESSEE

NO POSTAGE
NECESSARY
IF MAILED
IN THE
UNITED STATES

COMMANDING OFFICER
CODE L03
560 LABORATORY DRIVE
NAVAL CIVIL ENGINEERING LABORATORY
PORT HUENEME CA 93043-4328